Platelet activation stimulates macrophages to enhance ulcerative colitis through PF4/CXCR3 signaling

YUXIAO NIU[1,2*], ANHONG LI[2,3*], WEIHUA XU[4], RONG ZHANG[1,2], RUYA MEI[1,2], LANGHUA ZHANG[5], FENMIN ZHOU[6], QIN PAN[7] and YUZHONG YAN[1-3,8]

[1]Graduate School, Xinxiang Medical University, Xinxiang, Henan 453003, P.R. China; [2]Shanghai Key Laboratory of Molecular Imaging, Shanghai University of Medicine and Health Sciences, Zhoupu Hospital, Shanghai 201318, P.R. China; [3]Graduate School, Shanghai University of Traditional Chinese Medicine, Shanghai 200030, P.R. China; [4]Department of Pharmacy, Zhoupu Hospital, Shanghai University of Medicine and Health Sciences, Shanghai 201318, P.R. China; [5]School of Medical Technology, Shanghai University of Medicine and Health Sciences, Shanghai 201318, P.R. China; [6]Department of Traditional Chinese Medicine, Zhoupu Hospital, Shanghai University of Medicine and Health Sciences, Shanghai 201318, P.R. China; [7]Shanghai Institute of Pediatric Research, Shanghai Key Laboratory of Pediatric Gastroenterology and Nutrition, Shanghai 200092, P.R. China; [8]Department of Science Research, Zhoupu Hospital, Shanghai University of Medicine and Health Sciences, Shanghai 201318, P.R. China

Received November 21, 2024; Accepted February 19, 2025

DOI: 10.3892/ijmm.2025.5519

Abstract. Platelets are involved in hemostasis and immune regulation, but little is currently known regarding their role in inflammatory bowel disease. In the present study, the mechanism by which platelet activation affects macrophage C-X-C motif chemokine receptor 3 (CXCR3) by releasing platelet factor 4 (PF4), thus aggravating ulcerative colitis (UC) disease progression, was investigated. A dextran sulfate sodium-induced mouse model showed co-localization of the platelet marker PF4 with the macrophage M1 marker inducible nitric oxide synthase. Furthermore, co-culturing platelets with monocytes (THP-1) *in vitro* led to the transformation of monocytes into macrophages, as well as the activation of macrophages exhibiting proinflammatory properties. Meanwhile, reverse transcription-quantitative PCR (RT-qPCR) showed that inflammatory factors, such as IL-1β, IL-6 and TNF-α were significantly increased in macrophages after platelet co-culture. It was therefore hypothesized that the PF4/CXCR3 pathway may serve an important role in cell-to-cell communication. Furthermore, intervention with PF4 in THP-1 cells induced the M1 macrophage phenotype and inflammatory cytokine expression, which was consistent with co-culturing, whereas inhibition of CXCR3 (AMG487) reversed the effects of PF4. In addition, following treatment with PF4, THP-1 cells were found to be under oxidative stress and apoptosis was enhanced, as determined by detecting reactive oxygen species, mitochondrial membrane potential and Annexin-V, as well as the classical apoptotic proteins Bcl-2/Bax/caspase-3 through western blotting. In addition, changes in MAPK and NF-κB, two classic inflammatory signaling pathways, were detected. Furthermore, mice were treated with an anti-platelet medication or CXCR3 inhibitor to observe *in vivo* inflammatory changes; through phenotypic assessment, immunofluorescence staining, RT-qPCR and TUNEL assay, it was demonstrated that the PF4/CXCR3 pathway may aggravate inflammation in mice with UC. In conclusion, platelets and macrophages may interact in UC through the PF4/CXCR3 pathway to exacerbate inflammation, providing novel options for the treatment of UC.

Correspondence to: Dr Yuzhong Yan, Department of Science Research, Zhoupu Hospital, Shanghai University of Medicine and Health Sciences, 1500 Zhouyuan Road, Pudong, Shanghai 201318, P.R. China
E-mail: zp_yanyz@sumhs.edu.cn

Dr Qin Pan, Shanghai Institute of Pediatric Research, Shanghai Key Laboratory of Pediatric Gastroenterology and Nutrition, 1665 Kongjiang Road, Yangpu, Shanghai 200092, P.R. China
E-mail: pan_qin@yeah.net

*Contributed equally

Key words: platelet, macrophage, ulcerative colitis, platelet factor 4/C-X-C motif chemokine receptor 3, inflammation, apoptosis

Introduction

It has previously been shown that platelet activation is closely associated with inflammatory bowel disease (IBD), an autoimmune disorder that is associated with frequent relapses (1,2). As the disease progresses, tissue damage and microthrombi are common. Notably, mucosal capillary thrombosis can be detected in the rectal biopsy specimens of patients with IBD. Thrombosis mainly relies on platelet activation, indicating a close relationship between platelet activation and IBD (3). Furthermore, platelet aggregation and release are commonly observed on the colonic mucosa of patients with ulcerative colitis (UC) (4).

In the immune disease UC, chemokines such as platelet factor 4 (PF4) are released after platelet activation in the early

stages of inflammation, recruiting innate immune cells, such as macrophages. Macrophages serve an important role in maintaining intestinal immune homeostasis and have a notable effect on IBD, providing a promising opportunity for developing novel treatments (5). Notably, an association between platelets and macrophages has been reported in the context of sepsis, atherosclerosis and other diseases (6-8). Additionally, platelet-monocyte complexes (PMCs) have been shown to indicate the severity of various diseases (9), including UC (10).

Several cytokines are released after platelet activation, including PF4 (11). Atherosclerosis (12), as well as other diseases characterized by inflammation, induce the enhanced release of PF4 from platelets. In the pathogenesis of IBD, PF4 in plasma has also been reported to be increased (13) and to be associated with disease activity (14). C-X-C motif chemokine receptor 3 (CXCR3) is the receptor of PF4; PF4 recruits macrophages and binds to CXCR3, promoting macrophages to release proinflammatory factors. Furthermore, CXCR3 serves a notable role in the pathogenesis of UC; CXCR3 expression has been shown to be elevated in the peripheral blood and colon of patients with IBD (15), and CXCR3 axis expression is markedly higher in active IBD, indicating a role in its pathogenesis (16). Since CXCR3 attracts a multitude of proinflammatory cells, such as neutrophils, to the colon, inhibiting CXCR3 could be an effective means of regulating intestinal inflammation (17). CXCR3 is a receptor found in macrophages and other cell types (18), which has been demonstrated to have an inflammatory effect on immune cells via the NF-κB pathway (19) and Janus kinase/signal transducer and activator of transcription pathway (20). Moreover, CXCR3 has been shown to contribute to the pathogenesis of intestinal inflammation via the MAPK pathway. By contrast, inhibition of CXCR3 has been shown to confer protection against intestinal epithelial apoptosis (21). These previous findings suggest that PF4/CXCR3 may serve an important role in IBD.

Notably, there is evidence that the PF4/CXCR3 pathway is responsible for recruiting neutrophils, monocytes and lymphocytes (12,22), as well as polarizing macrophages and inducing cell fibrosis in the vascular wall (23). However, there is still a lack of understanding regarding the role of PF4/CXCR3 in IBD.

In the present study, the pivotal role of platelets and macrophages in UC was investigated, and the critical role of the PF4/CXCR3 pathway in the involvement of platelets and macrophages was investigated. It may be hypothesized that the current study could provide a solution to the issue of platelet regulation of macrophages through the PF4/CXCR3 pathway, which contributes to the progression of experimental colitis. Moreover, the findings may provide a feasible option for the treatment of UC.

Materials and methods

Patients. The current study was approved by the Ethics Committee of Zhoupu Hospital (approval no. ZPYYLL-2018-02; Shanghai, China) and was carried out in accordance with The Declaration of Helsinki. Three healthy male donors aged 54±14 years and three patients with UC (two male patients and one female patient) aged 34±19 years were selected for the present study. Peripheral colonic tissue from pediatric (age, <16 years) and adult subjects were collected after obtaining written informed consent from the patients or the pediatric patient's parent or guardian. The samples were collected during colonoscopy. The healthy donors underwent colonoscopy as part of a routine health check-up at the hospital. The patients with UC were diagnosed by a gastroenterologist and a pathologist. The puncture performed during colonoscopy yielded colon tissue, which underwent hematoxylin and eosin (H&E) staining and immunofluorescence detection using the following antibodies: Anti-CD62P (1:200; cat. no. 60322-1-Ig; Proteintech Group, Inc.), anti-inducible nitric oxide synthase (iNOS; 1:200; cat. no. 18985-1-AP; Proteintech Group, Inc.), anti-PF4 (1:100; cat. no. 21157-1-AP; Proteintech Group, Inc.) and anti-CXCR3 (1:100; cat. no. 26756-1-AP; Proteintech Group, Inc.).

Cell culture and treatment. THP-1 cells (cat. no. SCSP-567) were obtained from The Cell Bank of Type Culture Collection of The Chinese Academy of Sciences and were cultured in RPMI 1640 culture medium (cat. no. L210KJ; Shanghai Basalmedia Technologies Co., Ltd.) supplemented with 10% fetal bovine serum (cat. no. 098-150; Wisent, Inc.) and 1% penicillin-streptomycin (cat. no. 15140122; Gibco; Thermo Fisher Scientific, Inc.). The cells were maintained at 37˚C with 95% O_2 and 5% CO_2 in a humidified atmosphere. Phorbol 12-myristate 13-acetate (PMA), PF4, AMG487 (CXCR3 inhibitor), PD98059 (ERK inhibitor) and SC75741 (p65 inhibitor) were purchased from MedChemExpress (cat. nos. HY-18739, HY-P70618, HY-15319, HY-12028 and HY-10496, respectively). Lipopolysaccharide (LPS), which was used to induce the polarization of THP-1 cells to a proinflammatory phenotype, was purchased from Beijing Solarbio Science & Technology Co., Ltd. (cat. no. L8880). LPS (1 μg/ml) was added to THP-1 cells for 6 h at 37˚C and the samples were collected. PMA (100 ng/ml) was added to THP-1 cells for 24 h at 37˚C to induce the differentiation of monocytes into macrophages (24). After adding PMA to THP-1 cells to transform them into macrophages, the cells were treated as required. Subsequently, the samples were treated with AMG487 (2.5 μM) (25), PD98059 (10 μM) (26) or SC75741 (5 μM) (27) for 2 h at 37˚C, after which PF4 (100 ng/ml) was added for a further 6 h at 37˚C and the samples were collected.

Platelet isolation and culture-medium preparation. Human venous blood (5 ml) was collected from three of the aforementioned healthy volunteers at the Zhoupu Hospital Affiliated to Shanghai University of Medicine and Health Sciences (Shanghai, China). A portion of the blood was placed in a sodium citrate anticoagulant tube (BD Biosciences) and was subjected to centrifugation at 200 x g for 15 min at room temperature, thereby obtaining platelet-rich plasma (PRP). Prostaglandin 2 (500 ng/ml; Sigma-Aldrich; Merck KGaA) was added to PRP to prevent platelet activation. Platelet precipitation was carried out by centrifugation at 800 x g for 3 min at room temperature. The platelets were resuspended and washed in Tyrode's Salts buffer (140 mM NaCl, 10 mM $NaHCO_3$, 2.5 mM KCl, 0.5 mM Na_2HPO_4, 1 mM $MgCl_2$, 22 mM sodium citrate and 0.55 mM glucose; pH 6.5; Sigma-Aldrich; Merck KGaA), counted, and added to RPMI 1640 complete culture medium in an appropriate proportion for use (6). THP-1 cells were co-cultured with platelets at a ratio of 1:100 for 6 h. Light-field microscopic

observations were performed and images were captured using an inverted microscope (DMi1; Leica Biosystems).

Animals. A total of 20 healthy female Balb/c mice (age, 6-8 weeks; weight, 20-22 g) were provided by Hangzhou Qizhen Experimental Animal Technology Co., Ltd. The experimental procedure was conducted in accordance with the guidelines set by the National Institutes of Health (28), and all animal experiments were approved by the Animal Care and Use Professional Committee of Zhoupu Hospital (approval no. ZPYYLL-2018-02). The mice were maintained under the following controlled conditions: Temperature, 23±1˚C; humidity, 40-50%; 12-h light/dark cycle; *ad libitum* access to food and water. A 7-day acclimation period was allowed for the mice prior to the commencement of the study. The animals were euthanized if any case-predefined humane endpoints were observed, including: i) Weight loss, rapid loss of 15-20% of original body weight; ii) weakness, unable to eat and drink on their own, unable to stand for up to 24 h or unable to stand with extreme reluctance; and iii) signs of depression and hypothermia (<37˚C) without anesthesia or sedation. No humane endpoints were met throughout the experiments.

A murine model of dextran sulfate sodium (DSS)-induced acute colitis. A murine model of acute colitis was established by administering 2.5% DSS (Shanghai Yeasen Biotechnology Co., Ltd.) as previously described (29). The mice were randomly divided into the following four groups (n=5/group): Control, DSS, clopidogrel and AMG487 groups. Clopidogrel is a commonly used drug to inhibit platelet activation, and inhibition of platelet activation can reduce the production of platelet factors, including PF4. Following a 1-week period of acclimation, all experimental groups with the exception of the control group were administered a DSS solution, which was freshly prepared and replaced every other day, and the mice freely drank water mixed with DSS; mice were treated with AMG487 or clopidogrel (or control) for 3 days before DSS after the 1 week acclimation period. The clopidogrel group was administered an oral gavage of 20 mg/kg/day clopidogrel (MedChemExpress) (30,31), whereas the AMG487 group was administered an intraperitoneal injection of 5 mg/kg/day AMG487 (32). The control and DSS model groups were administered an intraperitoneal injection of a sterile PBS solution containing 20% β-cyclodextrin (MedChemExpress). The disease activity index (DAI) and histological examination (H&E staining) were used to assess the colitis model. DAI was scored as follows: Weight loss: 0, no weight loss; 1, 0-5%; 2, 5-10%; 3, 10-15%; 4, 15-20%. The degree of fecal softness: 0, no change; 1, soft stool; 2, loose stools. Fecal occult blood condition: 0, the color did not change within 2 min; 1, 1-2 min discoloration; 2, color change within 1 min; 3, discoloration within 10 sec; 4, immediate discoloration or hematochezia. The sum of the three scores is the DAI score. The fecal occult blood test was performed with the use of a fecal occult blood kit (cat. no. BA2020B; Baso Diagnostic, Inc.). Upon completion of the animal experiments, anesthesia was initiated with 3% isoflurane and was maintained with 1.5% isoflurane, and blood (0.5 ml) was taken from the apex of the heart, after which, the mice were euthanized with CO_2 at a volume replacement rate of 40% vol/min according to merican Veterinary Medical Association Guidelines for the Euthanasia of Animals: 2020 Edition (33). The colon was then removed for subsequent analysis. The blood samples were allowed to stand at room temperature for 60 min prior to centrifugation. After centrifugation at 2,000 x g for 15 min at room temperature, serum was obtained to assess the levels of inflammatory cytokines. The colon tissues were measured and washed to remove non-tissue debris. Subsequently, additional colon samples were stored at -80˚C for future analysis.

Histological scoring of colon tissues. Human and murine colon samples were sectioned after fixation with 4% paraformaldehyde for 24 h at room temperature and embedded in paraffin (Biosharp Life Sciences). The samples were then cut into 5-μm sections and mounted on slides. The sections were stained with H&E and then observed under a light microscope. Briefly, paraffin-embedded sections were oven-dried at 60˚C for 2 h, deparaffinized and stained with hematoxylin for 10 min, rinsed and stained with eosin for 30 sec, washed and sealed; the entire procedure was operated at room temperature. Two pathologists scored the extent of intestinal mucosal damage and inflammatory cell infiltration in a blinded manner. Briefly, in the case of damage to the intestinal mucosa, the following criteria were applied: 0, no damage; 1, discrete mucosal epithelial damage; 2, superficial mucosal erosion; 3, extensive mucosal damage. For crypt abnormalities, the following criteria were applied: 0, normal crypts; 1, a few crypts showed structural changes or atrophy; 2, structural changes or atrophy of numerous crypts; 3, extensive crypt abnormalities and loss. For inflammatory cell infiltration, the following criteria were applied: 0, none or a small amount of inflammatory cells in the lamina propria; 1, increased numbers of inflammatory cells in the lamina propria; 2, inflammatory cells spread to the submucosa; 3, the whole layer has inflammatory cell infiltration. The sum of the three scores was calculated as the colon histological score.

Reverse transcription-quantitative PCR (RT-qPCR). A total of 1x10^6 THP-1 cells/well were seeded into 6-well plates and divided into the following five experimental groups: i) Control group; ii) LPS group; iii) PLT group; iv) LPS + PLT group and v) LPS + PLT + $CaCl_2$ group. In the PLT groups, the THP-1 cells were co-cultured with platelets at a ratio of 1:100 for 6 h. In the LPS group, cells were collected 6 h after stimulation with LPS. In the LPS + PLT group, LPS was added during co-culture. In the LPS + PLT + $CaCl_2$ group, 10%w/v $CaCl_2$ was added to platelet conditioned medium for 5 min before co-culture with THP-1, and LPS was added at the same time. $CaCl_2$ is a commonly used platelet activator. All experiments were performed at 37˚C. In addition, PMA (100 ng/ml) was added to THP-1 cells for 24 h at 37˚C to induce the differentiation of monocytes into macrophages; these treatments are separate to the Control, LPS, PLT and LPS + PLT groups. After adding PMA to THP-1 cells to transform them into macrophages, experiments related to PF4/CXCR3 were performed. Subsequently, the samples were treated with AMG487 (2.5 μM/ml), PD98059 (10 μM) or SC75741 (5 μM) for 2 h at 37˚C, after which PF4 (100 ng/ml) (25) was added for a further 6 h at 37˚C and the samples were collected.

Total RNA was isolated from treated THP-1 cells and mouse colon tissue samples using TRIzol® (Invitrogen;

Table I. Primer sequences used for quantitative PCR.

A, Human primers

Gene	Forward primer, 5'-3'	Reverse primer, 5'-3'
GAPDH	GGAGCGAGATCCCTCCAAAAT	GGCTGTTGTCATACTTCTCTCATGG
IL-1β	ATGGCTTATTACAGTGGCAATGAGG	TGTAGTGGTGGTCGGAGATTCG
IL-6	TTCGGCAAATGTAGCATG	AATAGTGTCCTAACGCTCATAC
TNF-α	ATGAGCACTGAAAGCATGATCCG	AGGAGAAGAGGCTGAGGAACAAG
IL-10	CTTGCTGGAGGACTTTAAGGGTTAC	CTTGATGTCTGGGTCTTGGTTCTC
PF4	AACGGAGAGCCTGCTGAGTG	CCCAGACAGAAGTTGTTCTAACCAG
CXCR3	TGGTGGTGCTGGTGGACATC	GCCTGAGGTGACCGACTTGG
ERK	TGGTGTGCTCTGCTTATGATAATGTC	AGTAGGTCTGGTGCTCAAAGGG
P65	CCTGTCCTTTCTCATCCCATCTTTG	GCTGCCAGAGTTTCGGTTCAC
SRC	TCCAAGCCGCAGACTCAGG	CATCCACACCTCGCCAAAGC

B, Mouse primers

Gene	Forward primer, 5'-3'	Reverse primer, 5'-3'
GAPDH	AAGAAGGTGGTGAAGCAGG	GAAGGTGGAAGAGTGGGAGT
IL-1β	GAAATGCCACCTTTTGACAGTG	TGGATGCTCTCATCAGGACAG
IL-6	TAGTCCTTCCTACCCCAATTTCC	TTGGTCCTTAGCCACTCCTTC
TNF-α	CCGAGATGTGGAACTGGCAGAG	CCACGAGCAGGAATGAGAAGAGG
ZO-1	AGAGCAAGCCTTCTGCACAT	TCGGGTTTTCCCTTTGAAGAGT
OCLN	ACATGTATGGCGGAGAGATGC	GGGGCGACGTCCATTTGTAG
MUC-2	GAAGCCAGATCCCGAAACCA	GAATCGGTAGACATCGCCGT

PF4, platelet factor 4; CXCR3, C-X-C motif chemokine receptor 3; ZO-1, zonula occludens 1; OCLN, occludin; MUC-2, mucin 2.

Thermo Fisher Scientific, Inc.); briefly, the cells were washed with PBS, the supernatant was discarded and TRIzol was added for 10 min. Subsequently, chloroform was added and mixed vigorously for 30 sec, the supernatant was left for 10 min, and was then centrifuged at 12,000 x g for 15 min at 4˚C, and an equal volume of isopropanol was added for 10 min. After centrifugation at 12,000 x g for 15 min at 4˚C, the supernatant was discarded and then pre-cooled 75% ethanol was added to the remaining pellet. The RNA precipitate was obtained by centrifugation at 7,500 x g for 5 min at 4˚C and was resuspended in DEPC water. RNA at a final concentration of 1 μg was reverse transcribed into cDNA using a reverse transcriptase kit (Vazyme Biotech Co., Ltd). After mixing the relevant reagents of the kit, the samples were incubated at 50˚C for 15 min and 85˚C for 5 sec. qPCR was conducted on a Rotor-Gene Q-cycler (Qiagen, Inc.) using the Rotor-Gene SYBR Green qPCR Kit (Vazyme Biotech Co., Ltd.), according to the manufacturer's protocol. The thermocycling conditions were as follows: 95˚C for 30 sec, followed by 40 cycles at 95˚C for 10 sec and 60˚C for 30 sec; and final steps at 95˚C for 15 sec, 60˚C for 1 min and 95˚C for 15 sec. Human and mouse GAPDH were used as internal controls for parallel amplification. Relative changes in gene expression were quantified using the $2^{-\Delta\Delta Cq}$ method (34,35). All experiments were performed in triplicate. The specific primers (Sangon Biotech Co., Ltd.) used are listed in Table I. Among the specific primers, SRC was found in the 'Chemokine Signaling Pathway' and 'Cytokine-Cytokine Receptor Interaction' pathways when searching the downstream targets of PF4/CXCR3 in the Kyoto Encyclopedia of Genes and Genomes (KEGG) pathways (KEGG PATHWAY: map04062; https://www.genome.jp/entry/map04062 and KEGG PATHWAY: map04060; https://www.genome.jp/entry/map04060).

Western blotting. Total protein was isolated from THP-1 cells using RIPA buffer (Biosharp Life Sciences) containing protease and phosphatase inhibitors (Biosharp Life Sciences) on ice for 30 min. Subsequently, the cell fragments were centrifuged at 12,000 x g for 15 min at 4˚C. The soluble protein component was mixed with 5X loading buffer (Biosharp Life Sciences), and the concentration of proteins was determined using the BCA protein assay kit (Beyotime Institute of Biotechnology). Equal amounts of protein (30 μg/lane) were subjected to SDS-PAGE on 10 or 12.5% gels, and were electroblotted onto PVDF membranes (MilliporeSigma). The membranes were blocked using 5% fat-free milk (Beyotime Institute of Biotechnology) for 2 h at room temperature and were then incubated at 4˚C overnight with the following primary antibodies: Anti-CD62P (1:2,000; cat. no. 60322-1-Ig; Proteintech Group, Inc.), anti-inducible nitric oxide synthase (iNOS; 1:500; cat. no. 18985-1-AP; Proteintech Group, Inc.), anti-CD86 (1:500; cat. no. 26903-1-AP; Proteintech Group,

Inc.), anti-β-actin (1:20,000; cat. no. 66009-1-Ig; Proteintech Group, Inc.), anti-Bcl-2 (1:500; cat. no. 66799-1-Ig; Proteintech Group, Inc.), anti-Bax (1:1,000; cat. no. ET1603-34; HUABIO), anti-caspase-3 (1:1,000; cat. no. 14220; Cell Signaling Technology, Inc.), anti-ERK1/2 (1:1,000; cat. no. 4695; Cell Signaling Technology, Inc.), anti-phosphorylated (p)-ERK1/2 (1:2,000; cat. no. 4370; Cell Signaling Technology, Inc.), anti-p65 (1:1,000; cat. no. 6956; Cell Signaling Technology, Inc.) and anti-p-p65 (1:1,000; cat. no. 3033; Cell Signaling Technology, Inc.). After incubation with horseradish peroxidase-conjugated secondary antibodies (1:5,000; cat. nos. SA00001-1 and SA00001-2; Proteintech Group, Inc.) for 1 h at room temperature, the membranes were incubated with enhanced chemiluminescence (ECL) FemtoLight Substrate (cat. no. SQ201L; Epizyme; Ipsen Pharma). Protein detection was performed using the automatic chemiluminescence image analysis system (Tanon 5200 Multi; Tanon Science and Technology Co., Ltd.). Protein expression was semi-quantified using ImageJ (version 1.5.3; National Institutes of Health).

Flow cytometry. Apoptosis was detected by flow cytometry. After the cells were treated with 2.5 μM AMG487 for 2 h, 100 ng/ml PF4 was added for 24 h and the harvested cells were washed three times with PBS. Apoptosis was detected by flow cytometry after staining with Annexin V-FITC and PI (Beyotime Institute of Biotechnology) for 30 min at room temperature. The percentage of apoptotic cells was calculated, and the data were analyzed using Novo Express Immunofluorescence Analysis(version 1.4.1; Agilent Technologies, Inc.). The apoptotic rate was determined using a NovoCyte 2000 Flow Cytometer (Agilent Technologies, Inc.) (36).

Measurement of inflammatory cytokines. Mouse serum IL-1β and TNF-α levels were measured using an Automatic Biochemistry Analyzer (XPT; Siemens AG).

Reactive oxygen species (ROS) detection. ROS levels in THP-1 cells treated with PF4 and AMG487 were measured according to the instructions of the ROS kit (Beyotime Institute of Biotechnology). PMA (100 ng/ml) was added to THP-1 cells for 24 h at 37˚C to induce the differentiation of monocytes into macrophages. Subsequently, the samples were treated with AMG487 (2.5 μM) for 2 h at 37˚C, after which PF4 (100 ng/ml) was added for a further 24 h at 37˚C and the samples were collected. After washing with PBS, proportionally diluted DCFH-DA probes (in serum-free medium at a ratio of 1:1,000) were added to the cells. THP-1 cells were washed three times with PBS to completely remove the unbound DCFH-DA probe and were then fixed with 4% paraformaldehyde for 10 min at room temperature. After nuclear staining with DAPI, the intracellular ROS levels were assessed using ImageJ (version 1.5.3; National Institutes of Health) by detecting the fluorescence brightness of the DCFH-DA probe under FITC parameters. Imaging was performed using an inverted fluorescence microscope (DMi8; Leica Biosystems).

Mitochondrial membrane potential detection. The levels of JC-1 in THP-1 cells were determined in accordance with the instructions provided in the JC-1 kit (Beyotime Institute of Biotechnology). PMA (100 ng/ml) was added to THP-1 cells for 24 h at 37˚C to induce the differentiation of monocytes into macrophages. Subsequently, the samples were treated with AMG487 (2.5 μM) for 2 h at 37˚C, after which PF4 (100 ng/ml) was added for a further 6 h at 37˚C and the samples were collected. After washing with PBS, the JC-1 dye was added to the cells at a 1:200 dilution in JC-1 staining buffer and incubated at 37˚C for 20 min. Following two washes of the THP-1 cells with JC-1 staining buffer to ensure the complete elimination of unbound JC-1 dye, the intracellular mitochondrial membrane potential levels were evaluated using a fluorescence microscope. This involved the detection of the fluorescence intensities of both red and green fluorescence. Imaging was performed using an inverted fluorescence microscope (DMi8; Leica Biosystems).

Immunofluorescence staining analysis. For human and mouse colon tissue sample sections, immunostaining was performed using standard procedures. Briefly, human and murine colon samples were sectioned after fixation with 4% paraformaldehyde for 24 h at room temperature and embedded in paraffin (Biosharp Life Sciences). Paraffin-embedded 5-μm sections were dewaxed using xylene and rehydrated using gradient alcohol, and antigen repair was performed by microwave heating with Tris-EDTA (pH 9.0) at 95˚C for 20 min. The tissue was then blocked with 5% bovine serum albumin (cat. no. ST023; Beyotime Institute of Biotechnology) for 30 min at room temperature, after which the solution was removed and the sections were incubated overnight at 4˚C with the corresponding primary antibodies. The sections were then stained with TSA fluorescent labeling reagent (cat. no. bry-0023-100; Shanghai Ruiyu Biotechnology Co., Ltd.) for 30 min at room temperature and DAPI working solution (cat. no. P0131; Beyotime Institute of Biotechnology) was added dropwise. Imaging was carried out using a laser scanning confocal microscope (TCS SP8; Leica Biosystems). The antibodies used in this experiment included: Anti-CD62P (1:200; cat. no. 60322-1-Ig; Proteintech Group, Inc.), iNOS (1:100; cat. no. 18985-1-AP; Proteintech Group, Inc.), CD206 (1:200; cat. no. 18704-1-AP; Proteintech Group, Inc.), PF4 (1:100; cat. no. 21157-1-AP; Proteintech Group, Inc.) and CXCR3 (1:100; cat. no. 26756-1-AP; Proteintech Group, Inc.).

TUNEL assay. Briefly, human and murine colon samples were sectioned after fixation with 4% paraformaldehyde for 24 h at room temperature and embedded in paraffin. Paraffin-embedded mouse colon sections (5 μm) were dewaxed using xylene and rehydrated using gradient alcohol. Sample permeabilization was performed through incubation with 20 μg/ml proteinase K for 20 min at room temperature. Endogenous peroxidase was inactivated via incubation with 3% H_2O_2 for 5 min at room temperature. The TUNEL reaction mixture (cat. no. Roche-11684795910; Sigma-Aldrich; Merck KGaA) was added to the sample and incubated for 1 h at 37˚C. The DAPI working solution was added dropwise and imaging was carried out using a laser scanning confocal microscope (TCS SP8; Leica Biosystems).

Statistical analysis. Data are presented as the mean ± standard deviation (n≥3). Statistical analysis was performed using either unpaired, two-tailed Student's t-test, or one-way ANOVA

followed by Bonferroni post hoc test using GraphPad Prism (version 9.0; Dotmatics). Categorical data, such as DAI and pathological scores in animal experiments, are presented as the median (range) and were analyzed using the non-parametric Kruskal-Wallis test followed by Dunn's post hoc test. $P<0.05$ was considered to indicate a statistically significant difference.

Results

Platelets interact with monocytes and macrophages in UC, thereby facilitating the transformation of monocytes into macrophages that assume a proinflammatory role. In present study, it was observed that, compared with in the normal control group, in the colon of patients with UC, bleeding at the colonic mucosa was shown to occur during active UC (Fig. 1A). This was also observed in the colon of DSS-induced mice, with more neovascularization and microvessels, suggesting that platelets enter the colon from blood vessels and exert their effects (Fig. 1A and B). The co-localization of platelets and macrophages was investigated by staining for a platelet activation marker (CD62P) and a macrophage M1 marker (iNOS); the findings revealed that the co-localization of platelets with macrophages was more pronounced in the colon of patients with UC compared with in healthy controls (Fig. 1C). This finding was confirmed by staining for PF4 and iNOS in the mouse colon to detect the colocalization of platelets with proinflammatory macrophages (Fig. 1D).

In vitro, platelets were extracted from healthy individuals and co-cultured with THP-1 human monocytes. Observations at the microscopic level revealed that platelets contributed to the transformation of monocytes into macrophages, THP-1 cells were transformed from suspended monocytes into adherent macrophages (Fig. 2A). PMA, a common drug that induces mononuclear-to-macrophage transformation, was used as a reference group to verify THP-1 adherence. To examine the effects of platelets on macrophages in an inflammatory environment, an *in vitro* model of an inflammatory environment induced by LPS was developed. RT-qPCR confirmed that platelets facilitated the release of the proinflammatory cytokines IL-1β, IL-6 and TNF-α from monocyte-derived macrophages. Furthermore, in an LPS-induced proinflammatory environment, the addition of $CaCl_2$ to platelets resulted in a more pronounced inflammatory response. By contrast, platelets had little impact on the anti-inflammatory cytokine IL-10 (Fig. 2B). After co-culturing THP-1 cells with platelets, RT-qPCR demonstrated a notable increase in the expression of PF4 as well as CXCR3 compared with THP-1 cells only (Fig. 2C). According to these results, platelets may serve a key role in facilitating the differentiation of monocytes into macrophages and exerting proinflammatory effects.

Interaction between platelets and macrophages occurs via the PF4/CXCR3 pathway, which facilitates the polarization of macrophages towards the M1 phenotype. It was hypothesized that platelet activation could influence macrophages through the PF4/CXCR3 pathway, thereby affecting the progression of UC. Therefore, the CXCR3 inhibitor AMG487 was used during co-culture to validate its efficacy. As a result of the co-culture, the expression levels of CD62P, a platelet activation marker, and iNOS, a macrophage M1-type marker, were increased. In the presence of AMG487, iNOS expression was reduced, whereas the expression of CD62P was not affected (Fig. 3A). To better understand the role of this pathway, PF4 protein was added to THP-1 cells and the levels of inflammatory markers were measured. The results of RT-qPCR demonstrated that, as per the observations shown in Fig. 2B, the expression levels of inflammatory indicators, such as IL-1β, IL-6 and TNF-α, were elevated after the addition of PF4, whereas these expression levels were reduced following the addition of AMG487 (Fig. 3B).

According to the aforementioned findings, it was indicated that the addition of PF4 enhanced the M1 proinflammatory phenotype, as demonstrated by the M1 phenotypic markers CD86 and iNOS. Both CD86 and iNOS were upregulated after the addition of PF4 to THP-1 cells, whereas the inhibition of CXCR3 suppressed inflammation in macrophages (Fig. 3C). These results suggested that platelets interact with macrophages through the PF4/CXCR3 pathway, thereby promoting macrophage polarization towards a proinflammatory state.

PF4/CXCR3 is involved in the inflammatory response, and affects the oxidative stress and apoptosis of macrophages. ROS have been demonstrated to be associated with the development of inflammation. The levels of ROS were significantly elevated following the addition of PF4, whereas they were decreased following the addition of a CXCR3 inhibitor (Fig. 4A). Notably, the function of mitochondria can be impaired by excessive ROS; therefore, changes in the mitochondrial membrane potential were observed in macrophages following the addition of PF4 by JC-1 staining. When PF4 was added, the green fluorescence of the monomer was markedly increased, indicating a decrease in mitochondrial membrane potential, which AMG487 reversed (Fig. 4B). Reduced mitochondrial membrane potential can initiate the apoptosis signaling pathway; therefore, apoptosis was detected by Annexin-V FITC. FITC can be used to detect cells entering early apoptosis, PI detects cell necrosis, whereas cells positively stained for both FITC and PI are cells entering late apoptosis. FITC/PI staining was significantly increased following the addition of PF4, whereas this was reversed after the addition of AMG487 (Fig. 4C). To further clarify the regulatory factors of apoptosis, the key proteins involved in this process were detected. Compared with in the control group, the PF4 group exhibited significantly higher expression levels of the pro-apoptotic protein Bax, and lower expression levels of the anti-apoptotic protein Bcl-2, suggesting that PF4 increased apoptosis. In addition, caspase-3, which is a marker of irreversible apoptosis, was cleaved in response to PF4, whereas AMG487 reversed this effect (Fig. 4D).

PF4/CXCR3 pathway mediates the proinflammatory effect of macrophages through the MAPK and NF-κB pathways. The current study examined the regulatory function of PF4/CXCR3 by focusing on two established pathways associated with inflammatory processes: i) NF-κB and ii) MAPK. The protein expression levels of p-p65 and p-ERK were increased in response to PF4 and were decreased when CXCR3 was inhibited (Fig. 5A). To confirm this finding, the ERK inhibitor PD98059 and the p65 inhibitor SC75741 were used to treat the cells, and the inflammatory factors and macrophage M1

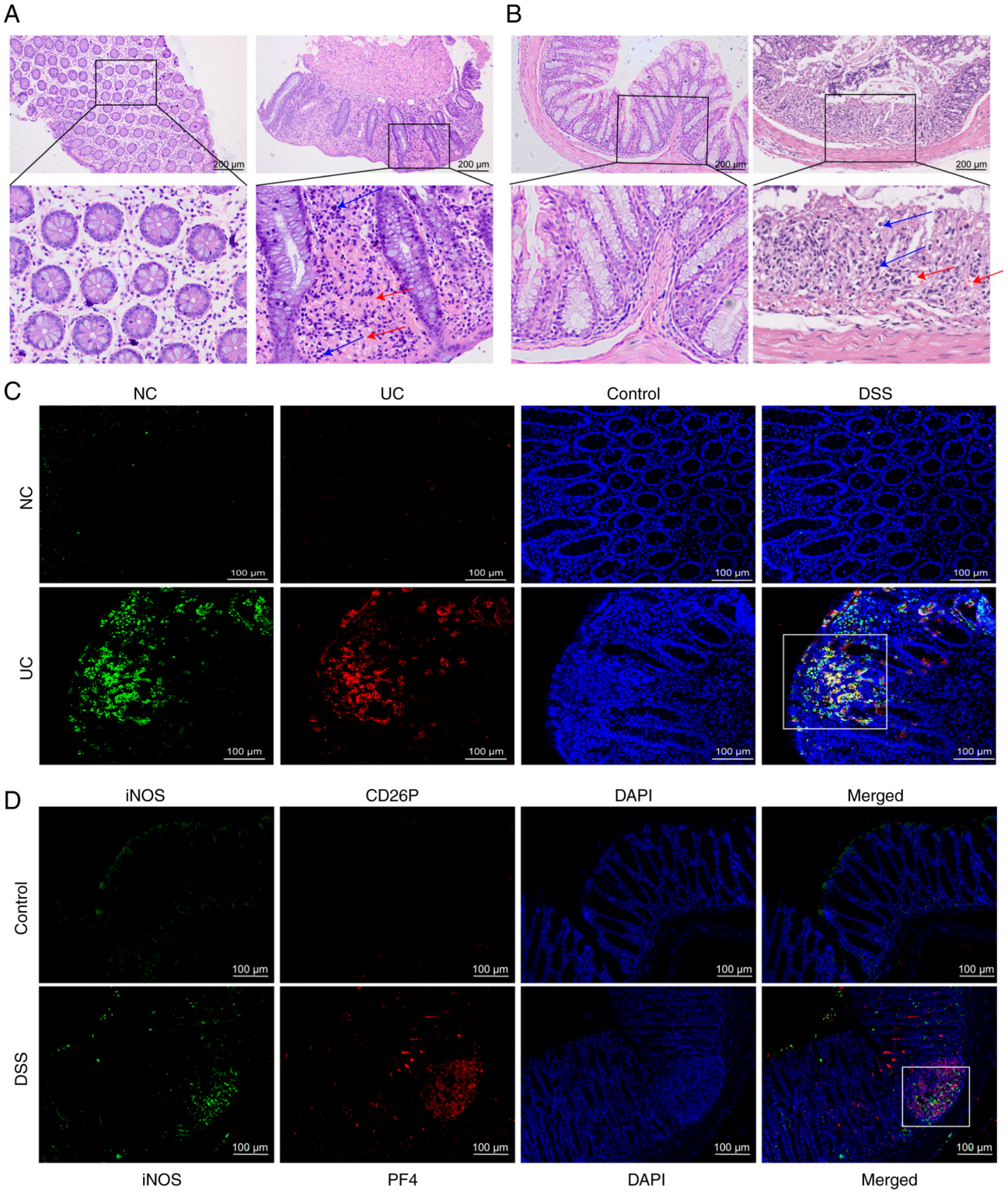

Figure 1. Colocalization of activated platelets and macrophages in UC. (A) Mucosal bleeding and inflammatory cell infiltration were observed in patients with UC compared with in normal human colon tissues. (B) DSS-induced UC in mice was characterized by mucosal hemorrhage and inflammatory cell infiltration compared with in control mice. (A and B) Red arrows indicate hemorrhage and blue arrows indicate inflammatory cell infiltration. Scale bars, 200 μm. (C) Co-localization of activated platelets (CD62P) and M1 macrophage (iNOS) markers was observed in the colonic mucosa compared with in the normal group. (D) Markers of activated platelets (PF4) and M1 macrophages (iNOS) showed colocalization in the colonic mucosa compared with in the control mice. Scale bars, 100 μm. NC, normal control; UC, ulcerative colitis; iNOS, inducible nitric oxide synthase; PF4, platelet factor 4; DSS, dextran sulfate sodium.

marker iNOS were subsequently detected, as well as another key gene downstream of CXCR3 and upstream of the two pathways, SRC. In the KEGG pathways 'Chemokine Signaling Pathway' and 'Cytokine-Cytokine Receptor Interaction', PF4 acts as a chemokine and activates downstream signals by binding to CXCR3. SRC may be involved in signal amplification and regulation downstream of CXCR3, and affect the activation and migration of immune cells. The results showed

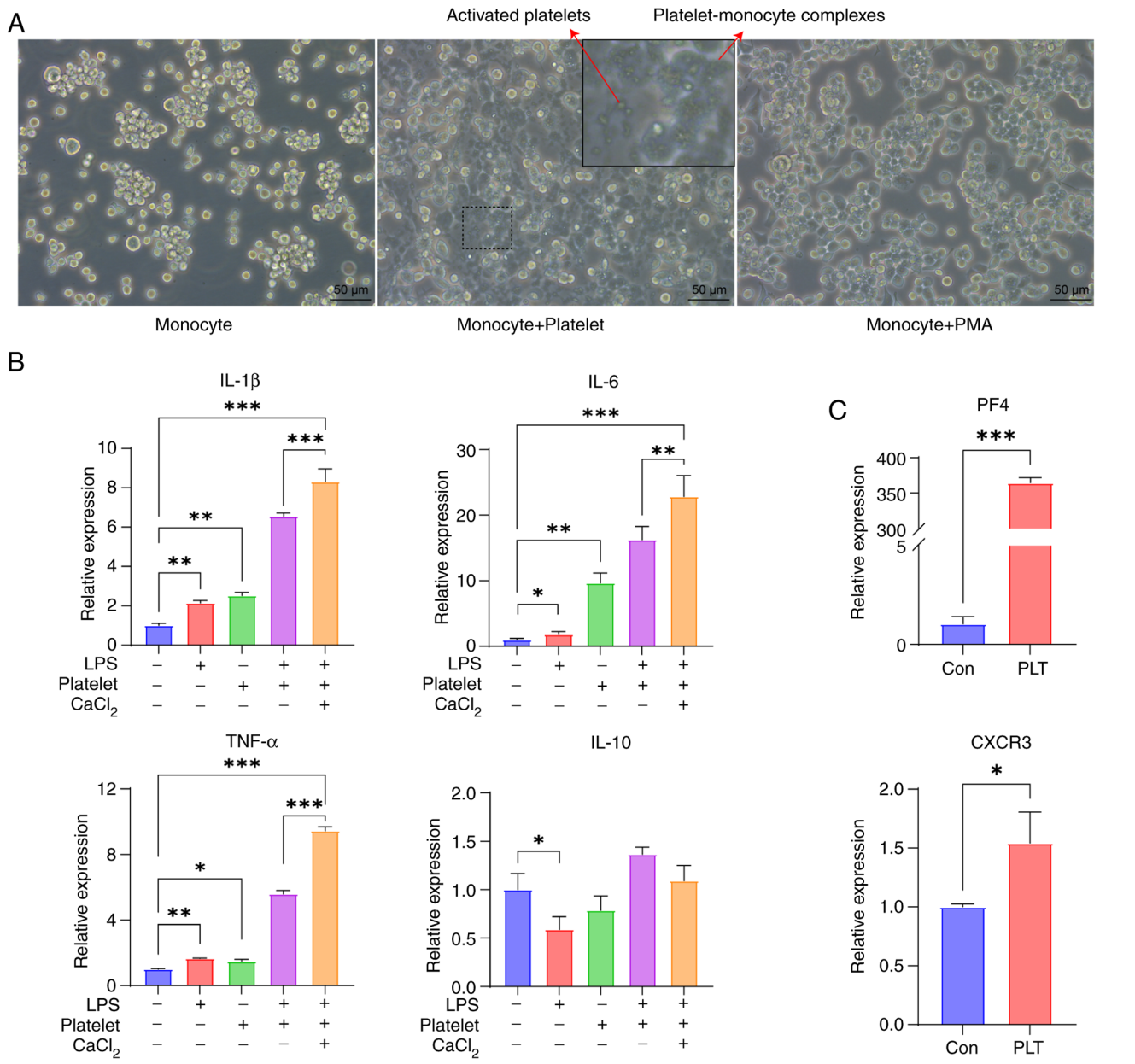

Figure 2. Co-culture of human platelets and macrophages induced platelet-derived PF4 release and an inflammatory response. (A) Morphological changes of macrophages after co-culture with platelets. Scale bar, 50 μm. (B) Changes in inflammatory factors were detected by qPCR following co-culture of THP-1 cells with platelets (n=3). (C) Changes in PF4/CXCR3 were detected by qPCR after THP-1 cells were co-cultured with platelets (n=3). Data are presented as the mean ± SD (n=3). *P<0.05, **P<0.01 and ***P<0.001. Con, THP-1 cells; PLT, THP-1 cells co-cultured with platelets; PF4, platelet factor 4; CXCR3, C-X-C motif chemokine receptor 3; qPCR, quantitative PCR; LPS, lipopolysaccharide; PMA, phorbol 12-myristate 13-acetate.

that the expression levels of iNOS, the M1 proinflammatory phenotypic marker, and ERK, p65 and SRC, the key genes of the two pathways, were decreased after the addition of the inhibitors, and the effect was equally efficacious when the two inhibitors were added together (Fig. 5B and C). Therefore, it was hypothesized that PF4/CXCR3 may regulate macrophage inflammation through the NF-κB and MAPK pathways.

Inhibition of platelet activation or CXCR3 improves disease progression in a DSS-induced mouse model of UC. The mice were treated with clopidogrel or AMG487 for 3 days prior to UC induction, followed by 7 days of free drinking of 2.5% DSS (Fig. 6A). During DSS administration, body weight was measured and fecal occult blood testing was performed daily, and the DAI score was calculated based on body weight change, fecal softness and occult blood conditions. Following the addition of DSS, the weight of mice decreased significantly, whereas the DAI score was significantly increased. Both the body weight and DAI of mice were significantly improved after administration of clopidogrel or AMG487 (Fig. 6B and C). The length of the colon is also a factor in determining UC. In the DSS group, the colon was significantly shortened, which was reversed in the clopidogrel and AMG487 groups (Fig. 6D). As a result of H&E staining, colon pathology was assessed and scored according to relevant inflammatory factors. The results indicated that the DSS group had the highest pathological score and the most severe disease, whereas clopidogrel and AMG487 effectively alleviated the condition (Fig. 6E).

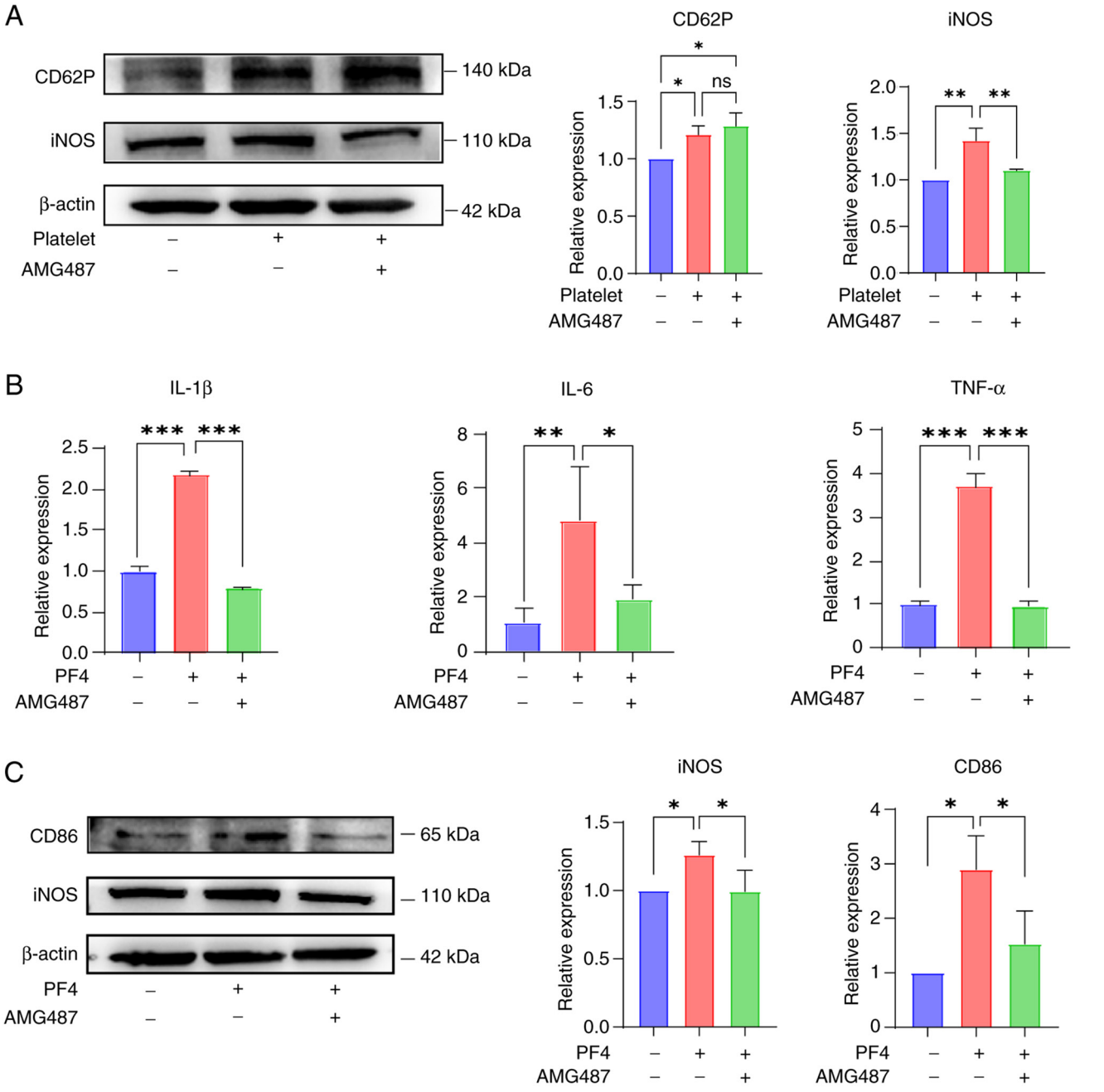

Figure 3. PF4/CXCR3 pathway promotes proinflammatory polarization of macrophages, and CXCR3 inhibition improves this effect. (A) Changes in the expression levels of iNOS and CD62P were detected by western blotting after the addition of platelets to THP-1 cells. (B) Changes in inflammatory factors were detected by quantitative PCR after adding PF4 to THP-1 cells. (C) Changes in CD86 and iNOS were detected by western blotting after adding PF4 to THP-1 cells. Data are presented as the mean ± SD (n=3). *P<0.05, **P<0.01 and ***P<0.001. PF4, platelet factor 4; CXCR3, C-X-C motif chemokine receptor 3; iNOS, inducible nitric oxide synthase; ns, not significant.

PF4/CXCR3 pathway aggravates the progression of UC, and blocking the release of PF4 from platelets or inhibiting CXCR3 can effectively inhibit UC. As a result of fluorescent double labeling of colon macrophage M1 and M2 markers (iNOS/CD206), an increase in M1 proinflammatory expression and a decrease in M2 expression in the mouse colon was observed after DSS stimulation, which was ameliorated by clopidogrel and AMG487 (Fig. 7A). As demonstrated by peripheral blood measurement of inflammatory cytokines and colon RT-qPCR, inflammation was elevated in the DSS group, which was ameliorated in the clopidogrel and AMG487 groups (Fig. 7B and C). Additionally, double labeling of PF4 and CXCR3 was performed. In the DSS group, confocal staining of PF4 and CXCR3 was detected, indicating that UC was aggravated by PF4/CXCR3 signaling in mice. Among the treatments administered, clopidogrel could inhibit the activation of platelets and reduce the content of PF4, whereas AMG487 inhibited CXCR3 expression (Fig. 7D). This finding was also confirmed by PF4/CXCR3 double labeling on colon samples from patients with UC (Fig. 7E).

TUNEL assay was then performed to detect apoptosis in mouse colons, and it was observed that apoptosis was markedly enhanced in the DSS group, whereas it was reduced in the clopidogrel and AMG487 groups (Fig. 8A). A similar pattern

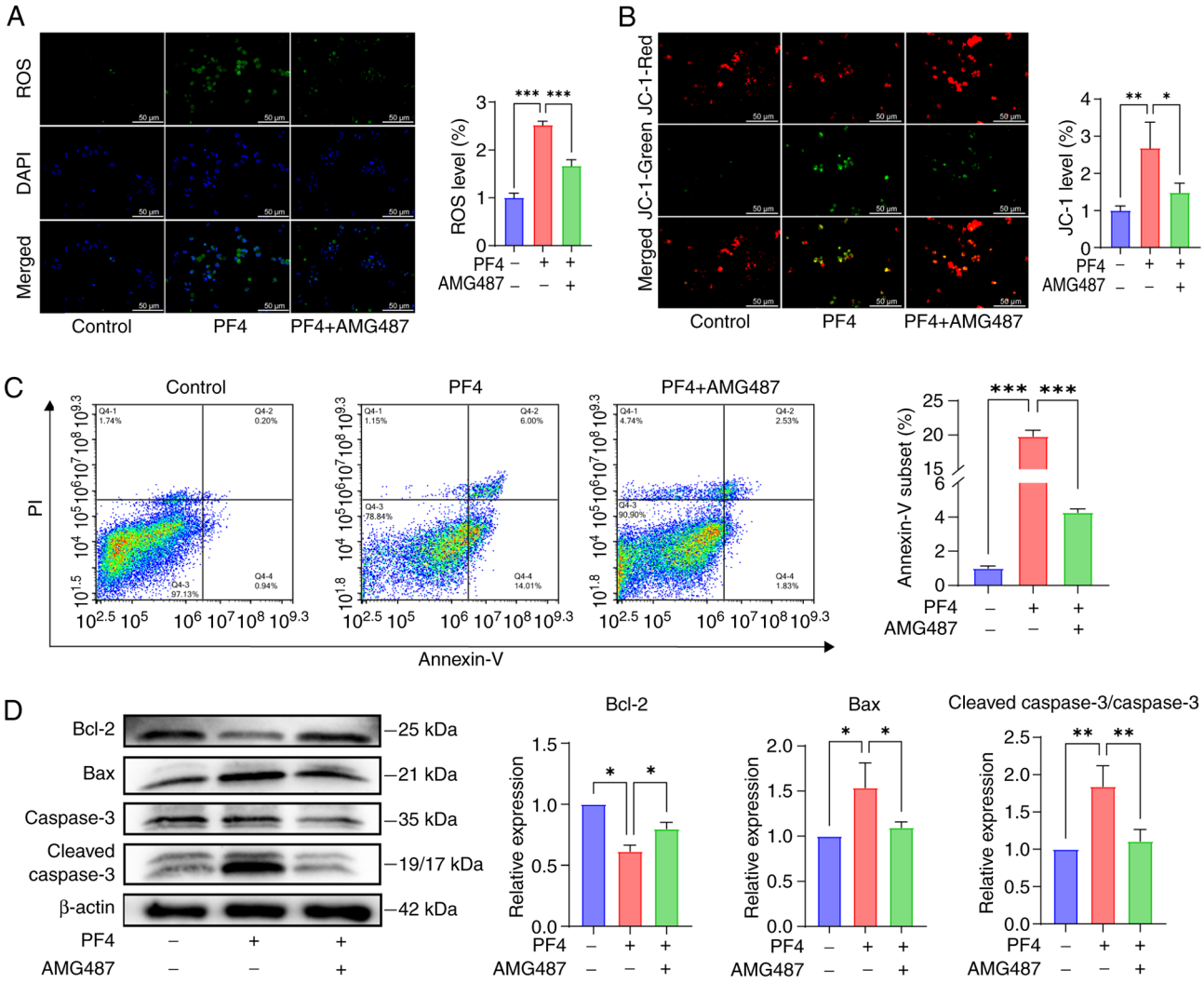

Figure 4. Apoptosis in macrophages is regulated through the PF4/CXCR3 pathway. (A) ROS levels in THP-1 cells after intervention with PF4 and CXCR3. Scale bar, 50 μm. (B) Representative fluorescence micrographs of mitochondrial membrane potential of THP-1 cells after PF4 and CXCR3 intervention; red represents normal mitochondrial membrane potential and green represents decreased membrane potential. Scale bar, 50 μm. (C) Flow cytometry was used to detect the apoptosis of THP-1 cells after PF4/CXCR3 intervention, where Annexin-V indicates apoptosis and PI indicates necrosis. (D) Expression levels of the apoptosis markers Bcl-2, Bax and caspase-3 in THP-1 cells after PF4/CXCR3 intervention was investigated by western blotting. Data are presented as the mean ± SD (n=3). *P<0.05, **P<0.01 and ***P<0.001. PF4, platelet factor 4; CXCR3, C-X-C motif chemokine receptor 3; ROS, reactive oxygen species.

of results was observed when tight junction proteins were used to measure the function of the colonic barrier. Zonula occludens 1, mucin 2 and occludin, which serve important roles in intestinal homeostasis, were stably expressed in the colon of the control group. Mice in the DSS group had severe colon tissue injury, and the expression levels of these genes were decreased; however, clopidogrel and AMG487 could alleviate colonic tissue damage and reverse these changes in expression levels (Fig. 8B). Thus, it was indicated that the PF4/CXCR3 pathway may be one of the key pathways in the progression of UC, which not only serves a key role in inflammatory progression, but also has a certain role in colonic apoptosis and intestinal barrier function.

PF4/CXCR3 pathway can affect disease progression through the NF-κB and MAPK pathways. The molecular mechanism through which platelets regulate macrophages through PF4/CXCR3 to enhance inflammation in UC was identified in the present study (Fig. 9). When UC develops, platelets bleed through vascular injury and enter the colon to activate platelets and release cytokines. PF4 released by platelets binds to the macrophage receptor CXCR3 in the colon, activating macrophages and polarizing them towards the proinflammatory phenotype through signaling pathways such as the MAPK and NF-κB pathways, serving a proinflammatory role and releasing proinflammatory factors. A variety of proinflammatory cells may be recruited into the colon by these inflammatory factors, causing inflammatory edema and affecting colon cell apoptosis. Under the influence of the PF4/CXCR3 pathway, macrophages are fully activated, ROS are released, mitochondrial function is disrupted and macrophage apoptosis is induced.

Discussion

IBD is an autoimmune disease that frequently recurs. In addition, it is common for tissue damage and microthrombus formation to occur during IBD. Platelets are associated with thrombosis, and have the potential to adhere and accumulate at the site of

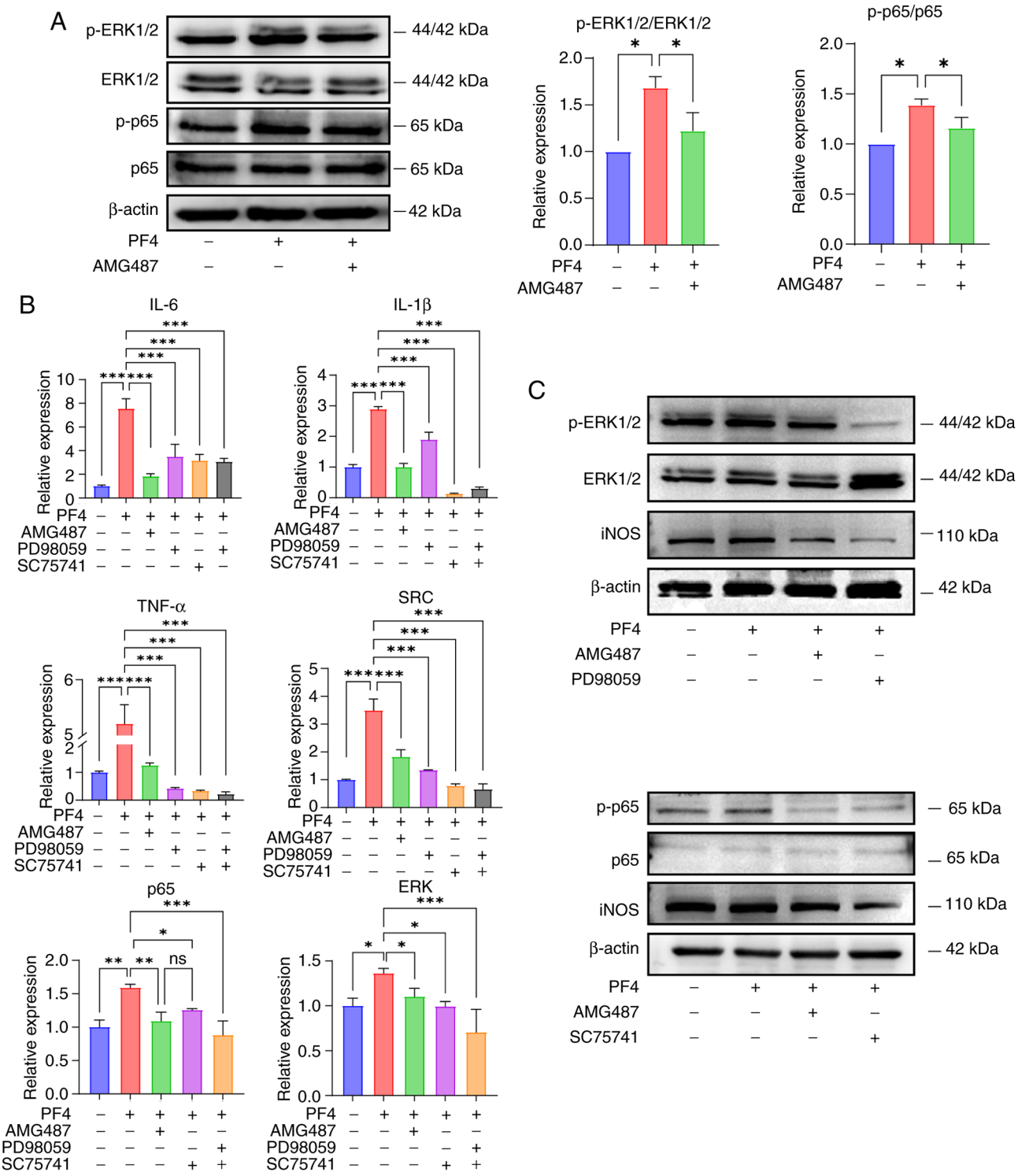

Figure 5. PF4/C-X-C motif chemokine receptor 3 pathway mediates the proinflammatory effects of macrophages through the MAPK and NF-κB pathways. (A) Expression levels of MAPK pathway markers (ERK) and NF-κB pathway markers (p65) in THP-1 cells were detected by western blotting after PF4 and AMG487 were added. (B) After adding the ERK inhibitor PD98059 and the p65 inhibitor SC75741, the expression levels of inflammatory factors (IL-1β, IL-6 and TNF-α), as well as the expression of SRC, ERK and P65 were detected by reverse transcription-quantitative PCR. (C) Changes in macrophage M1 markers (iNOS) and ERK/p65 after the addition of the two inhibitors. Data are presented as the mean ± SD (n=3). *P<0.05, **P<0.01 and ***P<0.001. PF4, platelet factor 4; iNOS, inducible nitric oxide synthase; p-, phosphorylated; ns, not significant.

vascular injury (1). In addition to repeated bleeding, UC is associated with common complications such as anemia and dysplasia. Through blood vessel bleeding, platelets enter the mucosal layer of the intestinal mucosa. Platelets also serve a significant role in inflammatory processes, infections and other diseases by interacting with, stimulating and regulating innate immune cells, such as neutrophils, monocytes and macrophages (37). It has been suggested that the megakaryocyte/platelet lineage may have evolved to coordinate the repair of vascular ruptures with the induction of an immune response (38).

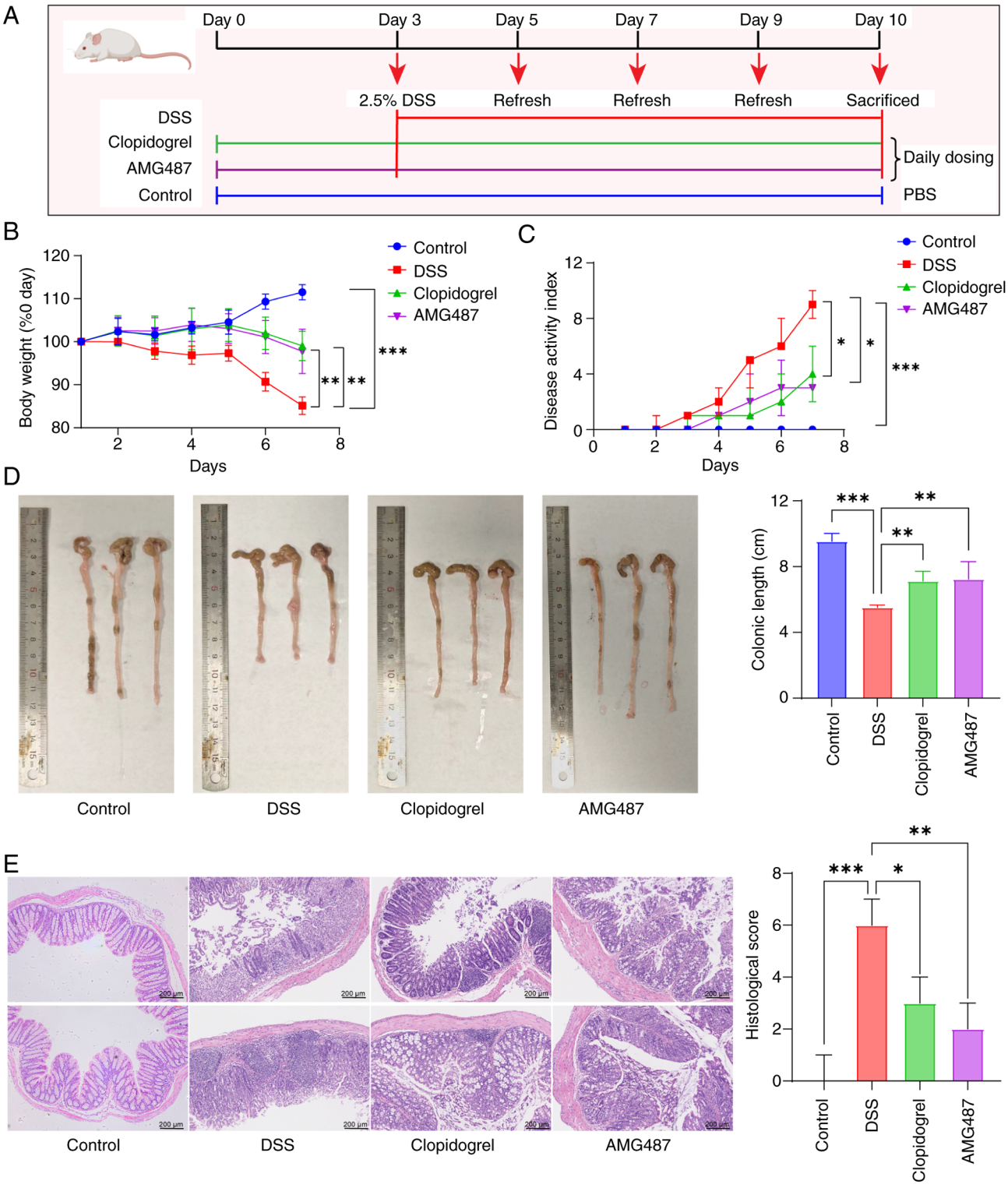

Figure 6. Platelet or C-X-C motif chemokine receptor 3 inhibition may prevent UC in mice. (A) Flow chart for modeling of UC in Balb/c mice; after 3 days of pretreatment with clopidogrel or AMG487, mice were given 2.5% DSS solution freely. The DSS solution was changed every 2 days and the mice were sacrificed on the last day of modeling. (B) Body weight of mice during DSS modeling was recorded daily. (C) Daily disease activity index score of mice during modeling, which was calculated according to changes in body weight, stool softness and fecal occult blood. (D) After modeling, the colon length of mice in each group was recorded and compared (n=5). (E) At the end of modeling, the colons were collected and pathological sections were made, and the pathological scores were calculated according to the degree of inflammatory cell infiltration, degree of crypt abnormality and degree of mucosal injury measured by hematoxylin and eosin staining. Scale bar, 200 μm. Continuous data are presented as the mean ± SD, whereas categorical data are presented as the median (range) (n=5). *P<0.05, **P<0.01 and ***P<0.001. UC, ulcerative colitis; DSS, dextran sulfate sodium.

CD62P and PF4 are the primary markers of platelet activation (39,40). The platelets in UC have a dual role in hemostasis and in the inflammatory response, interacting simultaneously with relevant immune cells in the colon. Macrophages represent a principal cell type of the intrinsic immune response and have been increasingly reported in UC in recent years (41).

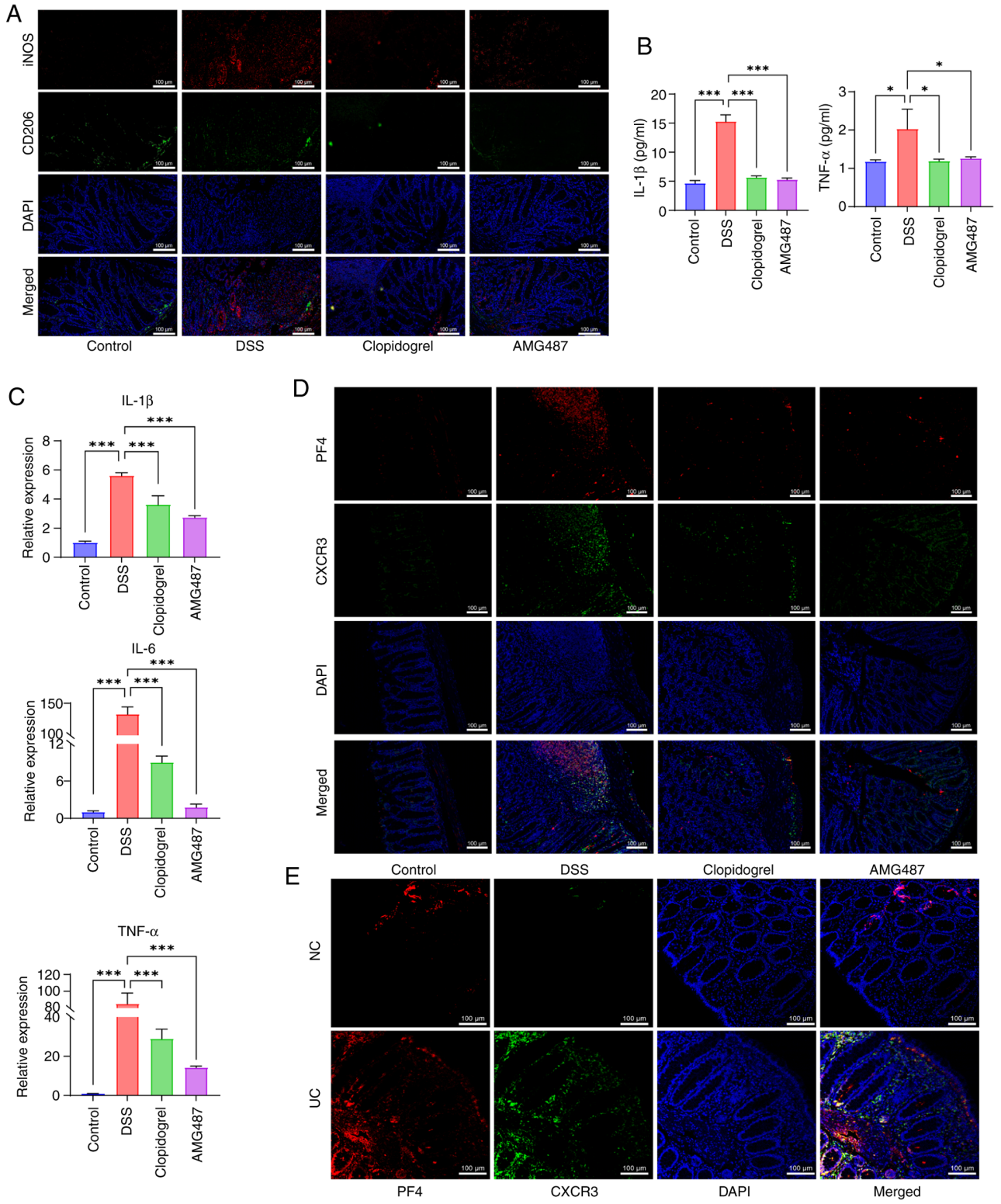

Figure 7. PF4/CXCR3 pathway affects the development of inflammation in a mouse model of UC. (A) Immunofluorescence visualization of M1 (iNOS)/M2 (CD206) expression in murine macrophages. Scale bar, 100 μm. (B) Changes in the serum levels of proinflammatory cytokines IL-1β and TNF-α in each group of mice (n=3). (C) Expression levels of mouse proinflammatory cytokines, IL-1β, IL-6 and TNF-α, were measured by reverse transcription-quantitative PCR in colon tissue (n=3). (D) Immunofluorescence detection of PF4/CXCR3 expression and distribution in mouse colon samples. Scale bar, 100 μm. (E) Immunofluorescence detection of PF4/CXCR3 expression and distribution in clinical colon samples. Scale bar, 100 μm. Data are presented as the mean ± SD (n=3). *P<0.05 and ***P<0.001. NC, normal control; UC, ulcerative colitis; PF4, platelet factor 4; CXCR3, C-X-C motif chemokine receptor 3; iNOS, inducible nitric oxide synthase; DSS, dextran sulfate sodium.

The majority of intestinal macrophages colonize the lamina propria of the mucosa, which is similar to the site of intestinal angiogenesis. It is reasonable to hypothesize that platelets and macrophages interact in the gut and stimulate each other. Once inflammation has begun, circulating monocytes leave the bloodstream and migrate to the tissues, where they undergo

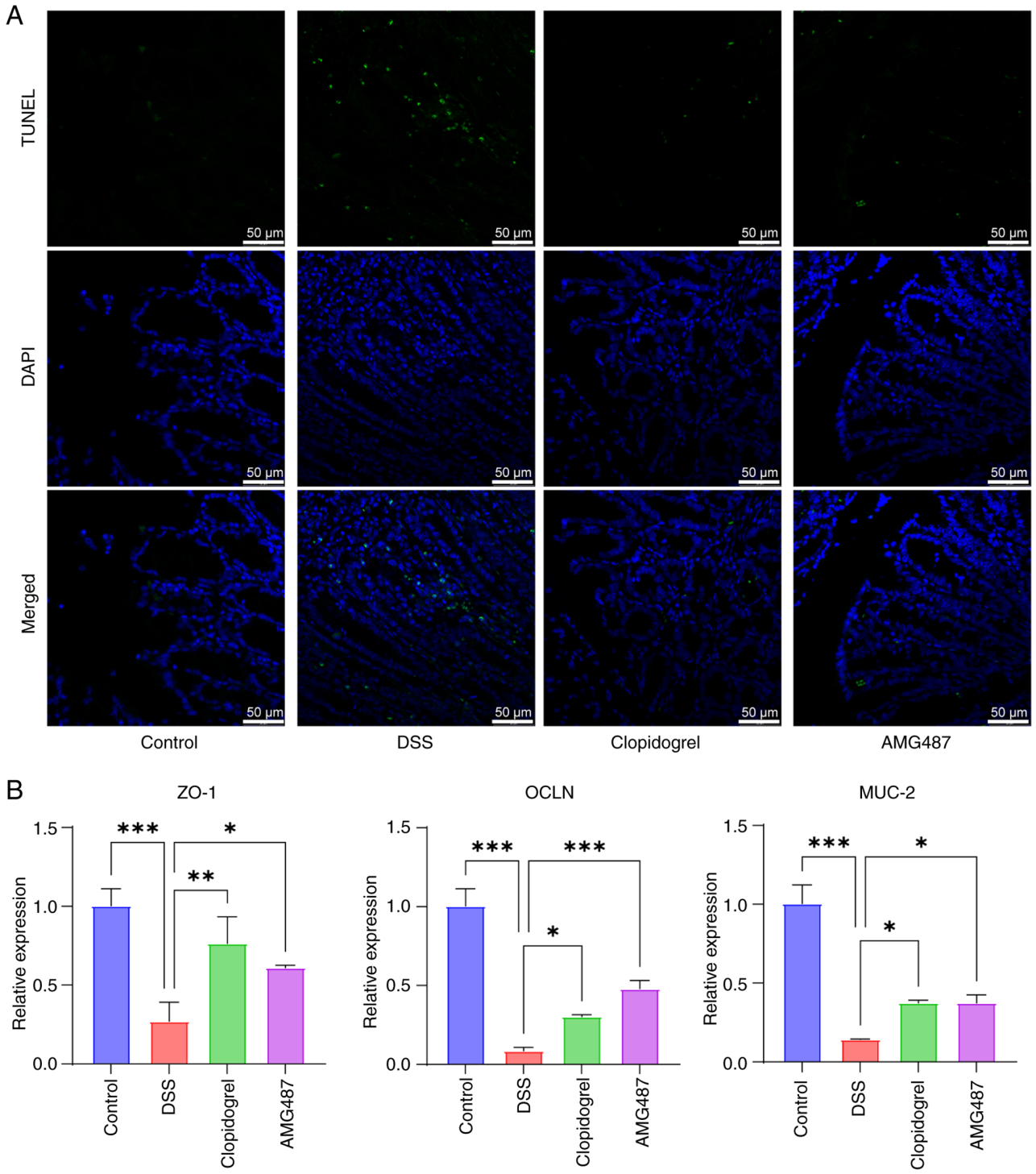

Figure 8. Platelet factor 4/C-X-C motif chemokine receptor 3 affects apoptosis and intestinal barrier protection in the colon. (A) Detection of apoptosis in mouse colon tissues by TUNEL staining. Scale bar, 50 μm. (B) Intestinal barrier dysfunction was detected by reverse transcription-quantitative PCR of tight junction markers (ZO-1, OCLN, MUC-2) (n=3). Data are presented as the mean ± SD (n=3). *P<0.05, **P<0.01 and ***P<0.001. ZO-1, zonula occludens 1; MUC-2, mucin 2; OCLN, occludin; DSS, dextran sulfate sodium.

differentiation in response to growth factors, cytokines or infection factors. This hypothesis is supported by previous studies that have demonstrated PMC formation in other diseases (42-45). Therefore, platelets and monocytes were co-cultured *in vitro* in the present study. The classical induction of monocyte-to-macrophage transformation with PMA was used as a reference point. As a result of the introduction of platelets, monocytes transitioned from suspension to apposition; monocytes are usually maintained in suspension. After stimulation, suspended cells can flow through blood vessels to the inflammatory site of tissues and transform into macrophages, which colonize and adhere to the inflammatory site. In addition, platelets attached to monocytes and formed PMCs.

During UC, platelets enter colonic tissue and release inflammatory factors, such as PF4 and TGF-β (4). As a result of this stimulation, macrophages release proinflammatory

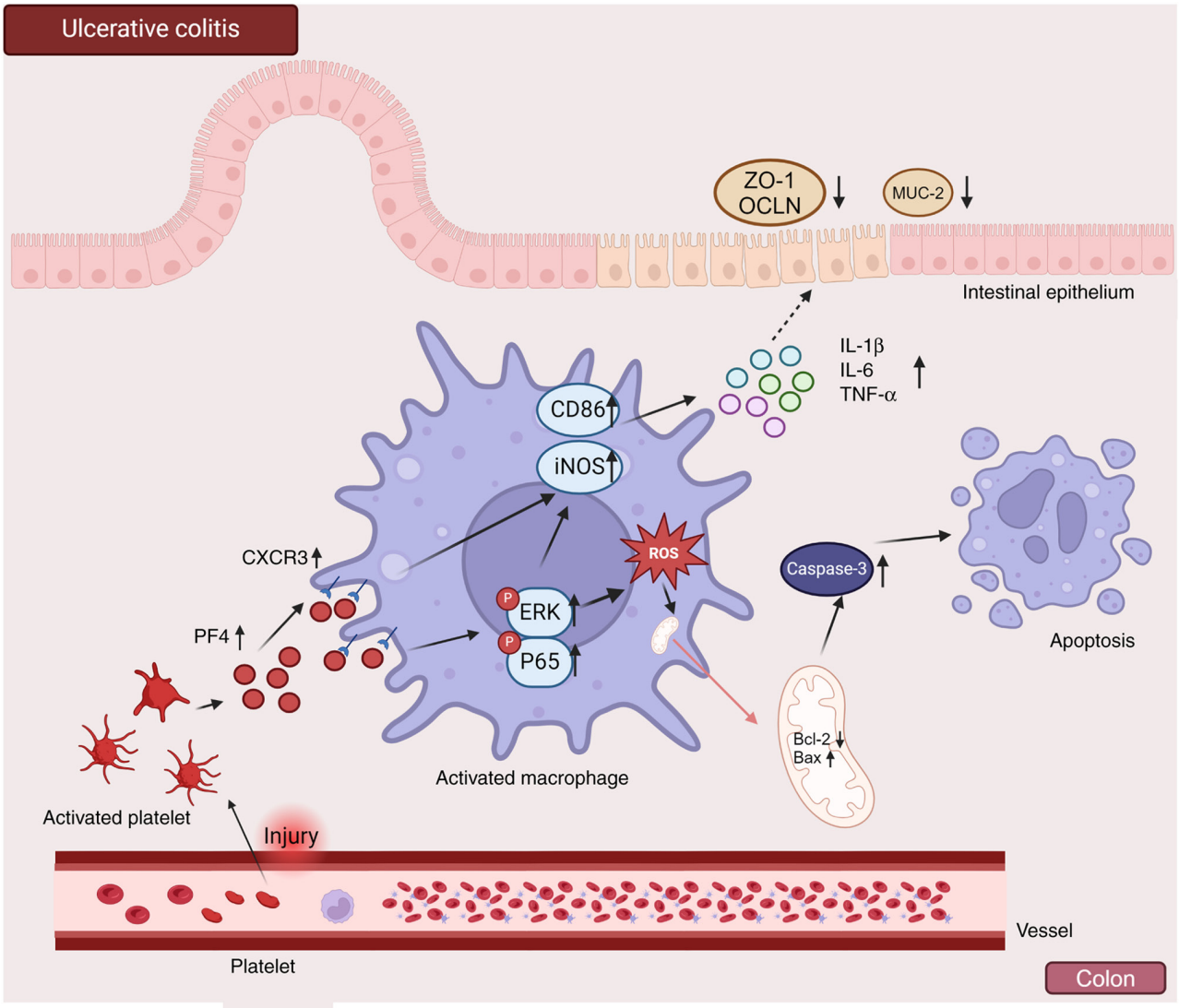

Figure 9. PF4/CXCR3 pathway can affect disease progression through NF-κB and MAPK pathways. Platelets regulate macrophages through PF4/CXCR3 to enhance the inflammatory response and promote macrophage apoptosis. Created in BioRender.com. PF4, platelet factor 4; CXCR3, C-X-C motif chemokine receptor 3; iNOS, inducible nitric oxide synthase; ZO-1, zonula occludens 1; MUC-2, mucin 2; OCLN, occludin.

cytokines, including IL-1β, IL-6 and TNF-α (46). The interaction between platelets and macrophages during inflammation was simulated *in vitro* in the present study; notably, after activating platelets with $CaCl_2$, the expression levels of proinflammatory cytokines were significantly increased, but the expression of IL-10, an anti-inflammatory factor, was not significantly affected. In addition, platelets may stimulate CXCR3 on mononuclear macrophages through the release of PF4 to activate macrophages and then serve a role in inflammatory responses. In the current study, the addition of the CXCR3 inhibitor AMG487 to the co-culture system demonstrated that platelets may promote inflammation by interacting with CXCR3. Despite this, platelets may have a bidirectional immunological function. It has been demonstrated that platelet derivatives, such as platelet lysate, can attenuate inflammation in the late stages of inflammation (47,48). Further investigation into these findings is thus warranted. Taken together, the present findings indicated that the two cell types may interact in UC, and this interaction could contribute to the exacerbation of inflammation at the onset of the disease.

Through PF4, platelets have an important role in a variety of diseases (49,50). The anticoagulant properties of PF4 are enhanced by its chemotactic effect on neutrophils and monocytes, which contributes to the immune response. In addition, PF4 inhibits the proliferation of endothelial cells, suggesting that it may be involved in the regulation of vascular processes (51). Through the release of PF4, platelets alter the phenotype of macrophages, thereby activating the differentiation of macrophages into proinflammatory cells; This unique subtype of macrophages mainly triggered by PF4 are known as M4 macrophages, which are clinically associated with inflammatory and fibrotic processes (22,52,53). CXCR3 is one of the main targets of PF4; notably, the CXCR3 axis serves an important role in the progression of IBD inflammation. In addition to CXCL9, CXCL10 and CXCL11, CXCR3 has numerous ligands that interfere with its expression. A growing number of studies have demonstrated that CXCL4 (PF4) binds to it as a ligand and induces targeted migration and immune responses (54-57). Therefore, the effects of PF4/CXCR3 on macrophages were investigated further. As a result of the

addition of PF4, macrophage inflammation was observed, which was consistent with the results of co-culture. These findings indicated that platelets may exert their proinflammatory effects on macrophages by activating them via the PF4/CXCR3 pathway.

The role of PF4/CXCR3 in inflammation has also been verified from a clinical aspect. PF4 binds to heparin to form an antigen, produces IgG antibodies and participates in heparin-induced thrombocytopenia. It has a variety of effects, including interference with platelet coagulation and promotion of host inflammatory response (58). A significant increase in PF4 has also been observed in the serum samples of patients with IBD (13). CXCR3 is expressed at high levels in macrophages and other adaptive immune cells are recruited by CXCR3. CXCR3 is expressed at high levels in Th1-Tc1 and Th17-Tc17 lymphocytes, and participate in cell migration to inflammatory tissues (59). The abundance of $HLA\text{-}DR^{+}CD38^{+}$ T cells, including T regulatory cells that produce inflammatory cytokines, $CXCR3^{+}$ plasmablasts and $IL1\beta^{+}$ macrophages and monocytes, has been shown to be increased in colonic mucosa samples from patients with IBD (60). This $CXCR3^{+}$ cell subpopulation serves an important role in the pathogenesis of human IBD (15,61). Studies have also been published on the role of the PF4/CXCR3 pathway in the context of inflammation, cardiovascular disease and aging (49,62). Taken together, these findings suggested that the PF4/CXCR3 signaling pathway may have an important role in the pathogenesis of IBD.

The mechanisms that promote the progression of inflammation were also examined in the present study. PF4/CXCR3 serves a significant role in ROS (63), apoptosis (64-66) and cell cycle progression. The apoptosis of macrophages may be initiated by a variety of factors during intestinal inflammation. Through a cascade of intracellular signaling pathways, pathogen infection may induce macrophages to initiate apoptotic programs. Additionally, various cytokines and chemical mediators released in an inflammatory milieu may disrupt macrophage homeostasis and trigger apoptosis. Moreover, macrophage survival may be affected by intercellular interactions, such as those with other immune cells (67,68). Chemokines, such as PF4, guide immune cells to areas of inflammation. Macrophages also serve a role in inflammation, engulfing pathogens and cytokines such as PF4 (25,49). In the present study, PF4 could enhance the production of ROS in macrophages, disrupting the balance between ROS production and clearance, resulting in excessive ROS accumulation and oxidative stress, whereas inhibiting CXCR3 decreased ROS levels. This enhanced oxidative stress induced by PF4 may damage mitochondria (69).

To determine whether mitochondrial function was impaired in the present study, a JC-1 assay was conducted. As a result of adding PF4, ROS levels were increased in macrophages, mitochondrial function was impaired and membrane potential was decreased, which was improved by inhibiting CXCR3. Mitochondrial membrane potential alterations are closely associated with the initial stages of apoptosis (70). In the present study, apoptosis was detected, and the results were consistent with those of previous studies (64,71,72). By inhibiting the pro-apoptotic protein Bax, Bcl-2 can protect cells from apoptosis. As a result of reduced or inhibited Bcl-2 protein levels, the pro-apoptotic cytoplasmic protein Bax enters mitochondria, disrupting the balance between pro-apoptotic and anti-apoptotic proteins, resulting in mitochondrial dysfunction and ultimately leading to macrophage apoptosis (73). PF4 increased ROS during inflammation, thus causing oxidative stress, which can activate pro-apoptotic proteins. Transfer of these molecules to the mitochondria results in a reduction in mitochondrial membrane potential and the subsequent opening of the mitochondrial permeability transition pore, which releases cytochrome *c* (Cyt C). This release of Cyt C triggers caspase-3 (74). A caspase cascade reaction ultimately results in a gradual increase in the externalization of phosphatidylserine, indicating irreversible apoptosis in macrophages (75,76).

In the present study, H&E staining of the colon in UC models demonstrated a marked reduction in crypts, an increase in inflammatory cell infiltration and almost complete loss of villi, all of which could be relieved by clopidogrel or AMG487. Pathological damage in UC may be explained by the presence of high levels of iNOS in the crypts of the colon, which may indicate that macrophages enter the crypts during inflammation and affect the growth of normal cells in the colon, thereby aggravating inflammation. Serum and colon cytokines were detected in the *in vivo* model, and it was also demonstrated that platelets can influence the polarization of macrophages and the release of inflammatory factors by releasing cytokines, thus affecting inflammation. It appears that PF4 and CXCR3 are clustered in areas of severe inflammation, and that the PF4/CXCR3 pathway may influence the severity of UC inflammation in mice.

As a result of UC, immune cells invade the crypts of the colon, causing cryptitis and crypt loss. The release of cytokines by platelets and macrophages during this time serves a key role in the progression of the disease. By releasing signals, macrophages recruit other immune cells to enter the colon and induce apoptosis, which interferes with the ability of the colon to repair its barrier (4,77). In murine UC, a strong association has been detected between TUNEL-positive cells and UC severity, indicating that apoptotic cell populations in colonic tissue may be linked to UC severity (78). In the present study, the TUNEL assay showed that this apoptosis was closely related to the PF4/CXCR3 pathway, and intervention with either of these factors could improve the development of UC. The tight junction index of the colon was also detected in the current study. In the mucosal epithelium, zonula occludens 1 maintains the mechanical barrier and permeability (79), occludin maintains tight junction stability (80) and mucin 2 is a type of mucin secreted by goblet cells. As the main component of intestinal mucus, mucin 2 contributes to maintenance of the intestinal barrier and the regulation of homeostasis (81,82). The levels of these three indicators were improved following treatment with clopidogrel and AMG487, indicating that platelets could alter intestinal barrier homeostasis through the PF4/CXCR3 pathway, thus aggravating UC.

There is evidence that PF4/CXCR3 modulates the inflammation of numerous cells by affecting pathways such as NF-κB, MAPK and others, which relates to immune dysfunction in UC (83,84). In the present study, P65 and ERK1/2 were detected after intervention of PF4 and CXCR3 *in vitro*, and the results demonstrated that PF4/CXCR3 significantly increased the

expression levels of P65 and ERK1/2, yielding results consistent with those observed in previous inflammation assays (85-88). In addition, the Kyoto Encyclopedia of Genes and Genomes pathways were searched and it was hypothesized that SRC might be a potential target downstream of the PF4/CXCR3 pathway. As a chemokine receptor, CXCR3 activates downstream effector molecules, including PI3K, MAPK and SRC family kinases, through G protein-mediated signaling (89,90). SRC serves a key role in downstream signaling of CXCR3 and regulates cell migration and inflammatory responses by phosphorylating downstream proteins (11,91). Notably, SRC was expressed in the 'Chemokine Signaling Pathway' and 'Cytokine-Cytokine Receptor Interaction' KEGG pathways. To fully demonstrate the role of these two pathways, inhibitors of the two pathways were used to mediate the PF4/CXCR3 pathway and the changes in inflammation were observed. The findings further confirmed that the PF4/CXCR3 pathway could upregulate the expression of inflammatory factors in macrophages through the NF-κB and MAPK signaling pathways, thereby aggravating inflammatory response and regulating apoptosis.

Notably, the present study has certain limitations. The DSS-induced UC mouse model is an acute model, which cannot fully mimic the long-term recurrent disease of human IBD. This limitation can be addressed by constructing animal models of chronic inflammation in future studies. Furthermore, the animal model was compared with patient colon samples, and the results showed some similarity, which will be refined in future studies. In future studies, this limitation could be addressed by collecting blood samples from patients to assess inflammatory factors and PF4 expression, and further studying inflammation and PF4/CXCR3 pathways in collected colon samples.

In conclusion, the THP-1 cell model induced by platelets and PF4, and the DSS-induced IBD mouse model revealed that platelet activation releases PF4, which may bind to macrophage CXCR3 and activate macrophages, polarizing them towards a proinflammatory phenotype, increasing the secretion of inflammatory factors, stimulating oxidative stress and apoptosis, and exhibiting proinflammatory effects. It may be possible to alleviate inflammation by inhibiting platelet activation or CXCR3 expression. In addition, there may be a notable role for MAPK or NF-κB signaling pathways in PF4/CXCR3 signaling. These findings provide an insight into the mechanisms by which PF4/CXCR3 promotes UC, and the current study provides experimental evidence that PF4/CXCR3 may be a promising therapeutic pathway for UC.

Acknowledgements

Not applicable.

Funding

The present study was supported by the Clinical Research Project of Shanghai University of Medicine and Health Sciences (grant no. 22MC2022002), the Research Grant for Pudong Health Bureau of Shanghai (grant no. YC-2023-0401), the Research Grant for Pudong Health Bureau of Shanghai (grant no. PW2024D-10), the Pudong New Area Science and Technology Commission (grant no. PKJ2023-Y109) and the Pudong New Area Science and Technology Commission (grant no. PKJ2021-Y32).

Availability of data and materials

The data generated in the present study may be requested from the corresponding author.

Authors' contributions

YZY, QP and YXN contributed to the research conception and design. YXN and AHL performed the experiments and drafted the manuscript. YZY, YXN and WHX confirm the authenticity of all the raw data. WHX, RZ, RYM, LHZ and FMZ performed data analysis and interpretation. All authors read and approved the final version of the manuscript.

Ethics approval and consent to participate

The present study was performed in line with the principles of The Declaration of Helsinki. The present study was approved by the Ethics Committee of Shanghai Zhoupu Hospital and the Animal Care and Use Professional Committee of Shanghai Zhoupu Hospital (approval no. ZPYYLL-2018-02). Written informed consent was obtained from all of the patients and the parents or guardians of the pediatric patients.

Patient consent for publication

Not applicable.

Competing interests

The authors declare that they have no competing interests.

References

1. van der Meijden PEJ and Heemskerk JWM: Platelet biology and functions: New concepts and clinical perspectives. Nat Rev Cardiol 16: 166-179, 2019.
2. Dhillon AP, Anthony A, Sim R, Wakefield AJ, Sankey EA, Hudson M, Allison MC and Pounder RE: Mucosal capillary thrombi in rectal biopsies. Histopathology 21: 127-133, 1992.
3. Custodio-Chablé SJ, Lezama RA and Reyes-Maldonado E: Platelet activation as a trigger factor for inflammation and atherosclerosis. Cir Cir 88: 233-243, 2020.
4. Huang B, Chen Z, Geng L, Wang J, Liang H, Cao Y, Chen H, Huang W, Su M, Wang H, *et al*: Mucosal profiling of pediatric-onset colitis and IBD reveals common pathogenics and therapeutic pathways. Cell 179: 1160-1176.e1124, 2019.
5. Pan X, Zhu Q, Pan LL and Sun J: Macrophage immunometabolism in inflammatory bowel diseases: From pathogenesis to therapy. Pharmacol Ther 238: 108176, 2022.
6. Carestia A, Mena HA, Olexen CM, Wilczyński JM, Negrotto S, Errasti AE, Gómez RM, Jenne CN, Silva EA and Schattner M: Platelets promote macrophage polarization toward pro-inflammatory phenotype and increase survival of septic mice. Cell Rep 28: 896-908.e895, 2019.
7. Laffont B, Corduan A, Rousseau M, Duchez AC, Lee CH, Boilard E and Provost P: Platelet microparticles reprogram macrophage gene expression and function. Thromb Haemost 115: 311-323, 2016.
8. Heffron SP, Weinstock A, Scolaro B, Chen S, Sansbury BE, Marecki G, Rolling CC, El Bannoudi H, Barrett T, Canary JW, *et al*: Platelet-conditioned media induces an anti-inflammatory macrophage phenotype through EP4. J Thromb Haemost 19: 562-573, 2021.

9. Rutten B, Tersteeg C, Vrijenhoek JE, van Holten TC, Elsenberg EH, Mak-Nienhuis EM, de Borst GJ, Jukema JW, Pijls NH, Waltenberger J, *et al*: Increased platelet reactivity is associated with circulating platelet-monocyte complexes and macrophages in human atherosclerotic plaques. PLoS One 9: e105019, 2014.
10. Pamuk GE, Vural O, Turgut B, Demir M, Umit H and Tezel A: Increased circulating platelet-neutrophil, platelet-monocyte complexes, and platelet activation in patients with ulcerative colitis: A comparative study. Am J Hematol 81: 753-759, 2006.
11. Kasper B and Petersen F: Molecular pathways of platelet factor 4/CXCL4 signaling. Eur J Cell Biol 90: 521-526, 2011.
12. Bakogiannis C, Sachse M, Stamatelopoulos K and Stellos K: Platelet-derived chemokines in inflammation and atherosclerosis. Cytokine 122: 154157, 2019.
13. Simi M, Leardi S, Tebano MT, Castelli M, Costantini FM and Speranza V: Raised plasma concentrations of platelet factor 4 (PF4) in Crohn's disease. Gut 28: 336-338, 1987.
14. Ye L, Zhang YP, Yu N, Jia YX, Wan SJ and Wang FY: Serum platelet factor 4 is a reliable activity parameter in adult patients with inflammatory bowel disease: A pilot study. Medicine (Baltimore) 96: e6323, 2017.
15. Mitsialis V, Wall S, Liu P, Ordovas-Montanes J, Parmet T, Vukovic M, Spencer D, Field M, McCourt C, Toothaker J, *et al*: Single-Cell analyses of colon and blood reveal distinct immune cell signatures of ulcerative colitis and Crohn's disease. Gastroenterology 159: 591-608.e510, 2020.
16. Schroepf S, Kappler R, Brand S, Prell C, Lohse P, Glas J, Hoster E, Helmbrecht J, Ballauff A, Berger M, *et al*: Strong overexpression of CXCR3 axis components in childhood inflammatory bowel disease. Inflamm Bowel Dis 16: 1882-1890, 2010.
17. Chami B, Yeung AW, van Vreden C, King NJ and Bao S: The role of CXCR3 in DSS-induced colitis. PLoS One 9: e101622, 2014.
18. Pandey V, Fleming-Martinez A, Bastea L, Doeppler HR, Eisenhauer J, Le T, Edenfield B and Storz P: CXCL10/CXCR3 signaling contributes to an inflammatory microenvironment and its blockade enhances progression of murine pancreatic precancerous lesions. Elife 10: e60646, 2021.
19. Zhang C, Deng Y, Zhang Y, Ba T, Niu S, Chen Y, Gao Y and Dai H: CXCR3 Inhibition blocks the NF-κB signaling pathway by elevating autophagy to ameliorate lipopolysaccharide-induced intestinal dysfunction in mice. Cells 12: 182, 2023.
20. Barone M, Catani L, Ricci F, Romano M, Forte D, Auteri G, Bartoletti D, Ottaviani E, Tazzari PL, Tazzari PL, *et al*: The role of circulating monocytes and JAK inhibition in the infectious-driven inflammatory response of myelofibrosis. Oncoimmunology 9: 1782575, 2020.
21. Gao J, Gao J, Qian L, Wang X, Wu M, Zhang Y, Ye H, Zhu S, Yu Y and Han W: Activation of p38-MAPK by CXCL4/CXCR3 axis contributes to p53-dependent intestinal apoptosis initiated by 5-fluorouracil. Cancer Biol Ther 15: 982-991, 2014.
22. Domschke G and Gleissner CA: CXCL4-induced macrophages in human atherosclerosis. Cytokine 122: 154141, 2019.
23. Hoeft K, Schaefer GJL, Kim H, Schumacher D, Bleckwehl T, Long Q, Klinkhammer BM, Peisker F, Koch L, Nagai J, *et al*: Platelet-instructed SPP1(+) macrophages drive myofibroblast activation in fibrosis in a CXCL4-dependent manner. Cell Rep 42: 112131, 2023.
24. Bohlen J, Zhou Q, Philippot Q, Ogishi M, Rinchai D, Nieminen T, Seyedpour S, Parvaneh N, Rezaei N, Yazdanpanah N, *et al*: Human MCTS1-dependent translation of JAK2 is essential for IFN-γ immunity to mycobacteria. Cell 186: 5114-5134.e5127, 2023.
25. Ojha A, Bhasym A, Mukherjee S, Annarapu GK, Bhakuni T, Akbar I, Seth T, Vikram NK, Vrati S, Basu A, *et al*: Platelet factor 4 promotes rapid replication and propagation of Dengue and Japanese encephalitis viruses. EBioMedicine 39: 332-347, 2019.
26. Hwang Y, Cha SH, Kim D and Jun HS: Combination of PD98059 and TGF-β1 efficiently differentiates human urine-derived stem cells into smooth muscle cells. Int J Mol Sci 22: 10532, 2021.
27. Tian B, Cai D, Wang M, He T, Deng L, Wu L, Jia R, Zhu D, Liu M, Chen S, *et al*: SC75741 antagonizes vesicular stomatitis virus, duck Tembusu virus, and duck plague virus infection in duck cells through promoting innate immune responses. Poult Sci 100: 101085, 2021.
28. National Research Council Committee for the Update of the Guide for the Care and Use of Laboratory Animal: The National academies collection: Reports funded by National Institutes of Health. In: Guide for the Care and Use of Laboratory Animals. National Academy of Sciences, Washington, DC, 2011.
29. Zeng B, Huang Y, Chen S, Xu R, Xu L, Qiu J, Shi F, Liu S, Zha Q, Ouyang D and He X: Dextran sodium sulfate potentiates NLRP3 inflammasome activation by modulating the KCa3.1 potassium channel in a mouse model of colitis. Cell Mol Immunol 19: 925-943, 2022.
30. Wang XL, Deng HF, Li T, Miao SY, Xiao ZH, Liu MD, Liu K and Xiao XZ: Clopidogrel reduces lipopolysaccharide-induced inflammation and neutrophil-platelet aggregates in an experimental endotoxemic model. J Biochem Mol Toxicol 33: e22279, 2019.
31. Korish AA: Clopidogrel prophylaxis abates myocardial ischemic injury and inhibits the hyperlipidemia-inflammation loop in hypercholestrolemic mice. Arch Med Res 51: 515-523, 2020.
32. Du J, Zhang X, Han J, Man K, Zhang Y, Chu ES, Nan Y and Yu J: Pro-Inflammatory CXCR3 impairs mitochondrial function in experimental non-alcoholic steatohepatitis. Theranostics 7: 4192-4203, 2017.
33. American Veterinary Medical Association (AVMA): AVMA guidelines for the euthanasia of animals: 2020 Edition. American Veterinary Medical Association, Schaumburg, IL, 2020.
34. Yang X, Liu Z, Zhou J, Guo J, Han T, Liu Y, Li Y, Bai Y, Xing Y, Wu J and Hu D: SPP1 promotes the polarization of M2 macrophages through the Jak2/Stat3 signaling pathway and accelerates the progression of idiopathic pulmonary fibrosis. Int J Mol Med 54: 89, 2024.
35. Livak KJ and Schmittgen TD: Analysis of relative gene expression data using real-time quantitative PCR and the 2(-Delta Delta C(T)) method. Methods 25: 402-408, 2001.
36. Liu X, Li J, Huang Q, Jin M and Huang G: Ginsenoside Rh2 shifts tumor metabolism from aerobic glycolysis to oxidative phosphorylation through regulating the HIF1-α/PDK4 axis in non-small cell lung cancer. Mol Med 30: 56, 2024.
37. Mandel J, Casari M, Stepanyan M, Martyanov A and Deppermann C: Beyond hemostasis: Platelet innate immune interactions and thromboinflammation. Int J Mol Sci 23: 3868, 2022.
38. Koupenova M, Livada AC and Morrell CN: Platelet and megakaryocyte roles in innate and adaptive immunity. Circ Res 130: 288-308, 2022.
39. Cibor D, Szczeklik K, Kozioł K, Pocztar H, Mach T and Owczarek D: Serum concentration of selected biochemical markers of endothelial dysfunction and inflammation in patients with the varying activity of inflammatory bowel disease. Pol Arch Intern Med 130: 598-606, 2020.
40. Takeyama H, Mizushima T, Iijima H, Shinichiro S, Uemura M, Nishimura J, Hata T, Takemasa I, Yamamoto H, Doki Y and Mori M: Platelet activation markers are associated with Crohn's disease activity in patients with low C-reactive protein. Dig Dis Sci 60: 3418-3423, 2015.
41. Zhang M, Li X, Zhang Q, Yang J and Liu G: Roles of macrophages on ulcerative colitis and colitis-associated colorectal cancer. Front Immunol 14: 1103617, 2023.
42. Rolling CC, Sowa MA, Wang TT, Cornwell M, Myndzar K, Schwartz T, El Bannoudi H, Buyon J, Barrett TJ and Berger JS: P2Y12 inhibition suppresses proinflammatory platelet-monocyte interactions. Thromb Haemost 123: 231-244, 2023.
43. Sano Y, Tomiyama T, Yagi N, Ito Y, Honzawa Y, Tahara T, Ikeura T, Fukui T, Shimoda S and Naganuma M: Platelet activation through CD62P and the formation of platelet-monocyte complexes are associated with the exacerbation of mucosal inflammation in patients with ulcerative colitis. Sci Rep 14: 28055, 2024.
44. Chao Y, Rebetz J, Bläckberg A, Hovold G, Sunnerhagen T, Rasmussen M, Semple JW and Shannon O: Distinct phenotypes of platelet, monocyte, and neutrophil activation occur during the acute and convalescent phase of COVID-19. Platelets 32: 1092-1102, 2021.
45. Tunjungputri RN, van de Heijden W, Urbanus RT, de Groot PG, van der Ven A and de Mast Q: Higher platelet reactivity and platelet-monocyte complex formation in Gram-positive sepsis compared to Gram-negative sepsis. Platelets 28: 595-601, 2017.
46. Tatiya-Aphiradee N, Chatuphonprasert W and Jarukamjorn K: Immune response and inflammatory pathway of ulcerative colitis. J Basic Clin Physiol Pharmacol 30: 1-10, 2018.
47. Kim JI, Bae HC, Park HJ, Lee MC and Han HS: Effect of storage conditions and activation on growth factor concentration in platelet-rich plasma. J Orthop Res 38: 777-784, 2020.
48. Nebie O, Barro L, Wu YW, Knutson F, Buée L, Devos D, Peng CW, Blum D and Burnouf T: Heat-treated human platelet pellet lysate modulates microglia activation, favors wound healing and promotes neuronal differentiation in vitro. Platelets 32: 226-237, 2021.

49. Schroer AB, Ventura PB, Sucharov J, Misra R, Chui MKK, Bieri G, Horowitz AM, Smith LK, Encabo K, Tenggara I, *et al*: Platelet factors attenuate inflammation and rescue cognition in ageing. Nature 620: 1071-1079, 2023.
50. Liu Z, Li L, Zhang H, Pang X, Qiu Z, Xiang Q and Cui Y: Platelet factor 4(PF4) and its multiple roles in diseases. Blood Rev 64: 101155, 2024.
51. Yang C, Bachu M, Du Y, Brauner C, Yuan R, Ah Kioon MD, Chesi G, Barrat FJ and Ivashkiv LB: CXCL4 synergizes with TLR8 for TBK1-IRF5 activation, epigenomic remodeling and inflammatory response in human monocytes. Nat Commun 13: 3426, 2022.
52. Yu B, Jia S, Chen Y, Guan R, Chen S, Tang W, Bao T and Tian Z: CXCL4 deficiency limits M4 macrophage infiltration and attenuates hyperoxia-induced lung injury. Mol Med 30: 253, 2024.
53. Li H, Cao Z, Wang L, Liu C, Lin H, Tang Y and Yao P: Macrophage subsets and death are responsible for atherosclerotic plaque formation. Front Immunol 13: 843712, 2022.
54. Wang K, Wu J, Yang Z, Zheng B, Shen S, Wang RR, Zhang Y, Wang HY, Chen L and Qiu X: Hyperactivation of β-catenin signal in hepatocellular carcinoma recruits myeloid-derived suppressor cells through PF4-CXCR3 axis. Cancer Lett 586: 216690, 2024.
55. Kuratani A, Okamoto M, Kishida K, Okuzaki D, Sasai M, Sakaguchi S, Arase H and Yamamoto M: Platelet factor 4-induced T(H)1-T(reg) polarization suppresses antitumor immunity. Science 386: eadn8608, 2024.
56. Tan S, Li S, Min Y, Gisterå A, Moruzzi N, Zhang J, Sun Y, Andersson J, Malmström RE, Wang M, *et al*: Platelet factor 4 enhances CD4(+) T effector memory cell responses via Akt-PGC1α-TFAM signaling-mediated mitochondrial biogenesis. J Thromb Haemost 18: 2685-2700, 2020.
57. Tan S, Zhang J, Sun Y, Gisterå A, Sheng Z, Malmström RE, Hou M, Peng J, Ma C, Liao W and Li N: Platelets enhance CD4+ central memory T cell responses via platelet factor 4-dependent mitochondrial biogenesis and cell proliferation. Platelets 33: 360-370, 2022.
58. Arepally GM: Heparin-induced thrombocytopenia. Blood 129: 2864-2872, 2017.
59. Alfaro R, Llorente S, Gonzalez-Martínez G, Jimenez-Coll V, Martínez-Banaclocha H, Galián JA, Botella C, Moya-Quiles MR, de la Peña-Moral J, Minguela A, *et al*: Clinical significance of the pre-transplant CXCR3 and CCR6 expression on T cells in kidney graft recipients. Transplant Proc 55: 66-71, 2023.
60. Wang S, Zhang Y, Chen G, Zhao P, Wang X, Xu B and Yuan L: Expressions of CXCR3 and PD-1 on T cells and their clinical relevance in colorectal cancer. Int Immunopharmacol 132: 111988, 2024.
61. Papadakis KA, Prehn J, Zhu D, Landers C, Gaiennie J, Fleshner PR and Targan SR: Expression and regulation of the chemokine receptor CXCR3 on lymphocytes from normal and inflammatory bowel disease mucosa. Inflamm Bowel Dis 10: 778-788, 2004.
62. Altara R, Manca M, Brandão RD, Zeidan A, Booz GW and Zouein FA: Emerging importance of chemokine receptor CXCR3 and its ligands in cardiovascular diseases. Clin Sci (Lond) 130: 463-478, 2016.
63. Zhou H, Deng M, Liu Y, Yang C, Hoffman R, Zhou J, Loughran PA, Scott MJ, Neal MD and Billiar TR: Platelet HMGB1 is required for efficient bacterial clearance in intra-abdominal bacterial sepsis in mice. Blood Adv 2: 638-648, 2018.
64. Woller G, Brandt E, Mittelstädt J, Rybakowski C and Petersen F: Platelet factor 4/CXCL4-stimulated human monocytes induce apoptosis in endothelial cells by the release of oxygen radicals. J Leukoc Biol 83: 936-945, 2008.
65. Pervushina O, Scheuerer B, Reiling N, Behnke L, Schröder JM, Kasper B, Brandt E, Bulfone-Paus S and Petersen F: Platelet factor 4/CXCL4 induces phagocytosis and the generation of reactive oxygen metabolites in mononuclear phagocytes independently of Gi protein activation or intracellular calcium transients. J Immunol 173: 2060-2067, 2004.
66. Saahene RO, Wang J, Wang ML, Agbo E and Pang D: The anti-tumor mechanism of paeonol on CXCL4/CXCR3-B signals in breast cancer through induction of tumor cell apoptosis. Cancer Biother Radiopharm 33: 233-240, 2018.
67. Liu X, Zhou M, Dai Z, Luo S, Shi Y, He Z and Chen Y: Salidroside alleviates ulcerative colitis via inhibiting macrophage pyroptosis and repairing the dysbacteriosis-associated Th17/Treg imbalance. Phytother Res 37: 367-382, 2023.
68. Pedersen J, LaCasse EC, Seidelin JB, Coskun M and Nielsen OH: Inhibitors of apoptosis (IAPs) regulate intestinal immunity and inflammatory bowel disease (IBD) inflammation. Trends Mol Med 20: 652-665, 2014.
69. Deng Z, Liu Q, Wang M, Wei HK and Peng J: GPA Peptide-Induced Nur77 localization at mitochondria inhibits inflammation and oxidative stress through activating autophagy in the intestine. Oxid Med Cell Longev 2020: 4964202, 2020.
70. Xiao JJ, Liu Q, Li Y, Peng FF, Wang S, Zhang Z, Liu H, Yu H, Tao S and Zhang BF: Regulator of calcineurin 1 deletion attenuates mitochondrial dysfunction and apoptosis in acute kidney injury through JNK/Mff signaling pathway. Cell Death Dis 13: 774, 2022.
71. Xu W, Ye S, Liu W, Guo H, Zhang L, Wei S, Anwaier A, Chang K, Malafaia G, Zhang H, *et al*: Single-cell RNA-seq analysis decodes the kidney microenvironment induced by polystyrene microplastics in mice receiving a high-fat diet. J Nanobiotechnology 22: 13, 2024.
72. Nevzorova TA, Mordakhanova ER, Daminova AG, Ponomareva AA, Andrianova IA, Le Minh G, Rauova L, Litvinov RI and Weisel JW: Platelet factor 4-containing immune complexes induce platelet activation followed by calpain-dependent platelet death. Cell Death Discov 5: 106, 2019.
73. Kulyar MF, Yao W, Ding Y, Du H, Li K, Zhang L, Li A, Huachun P, Waqas M, Mehmood K and Li J: Cluster of differentiation 147 (CD147) expression is linked with thiram induced chondrocyte's apoptosis via Bcl-2/Bax/Caspase-3 signalling in tibial growth plate under chlorogenic acid repercussion. Ecotoxicol Environ Saf 213: 112059, 2021.
74. Ali N, Rashid S, Nafees S, Hasan SK, Shahid A, Majed F and Sultana S: Protective effect of Chlorogenic acid against methotrexate induced oxidative stress, inflammation and apoptosis in rat liver: An experimental approach. Chem Biol Interact 272: 80-91, 2017.
75. Yang C, Wang ZQ, Zhang ZC, Lou G and Jin WL: CBL0137 activates ROS/BAX signaling to promote caspase-3/GSDME-dependent pyroptosis in ovarian cancer cells. Biomed Pharmacother 161: 114529, 2023.
76. Zhang Y, Yang X, Ge X and Zhang F: Puerarin attenuates neurological deficits via Bcl-2/Bax/cleaved caspase-3 and Sirt3/SOD2 apoptotic pathways in subarachnoid hemorrhage mice. Biomed Pharmacother 109: 726-733, 2019.
77. Hu Q, Lyon CJ, Fletcher JK, Tang W, Wan M and Hu TY: Extracellular vesicle activities regulating macrophage- and tissue-mediated injury and repair responses. Acta Pharm Sin B 11: 1493-1512, 2021.
78. Wu MY, Liu L, Wang EJ, Xiao HT, Cai CZ, Wang J, Su H, Wang Y, Tan J, Zhang Z, *et al*: PI3KC3 complex subunit NRBF2 is required for apoptotic cell clearance to restrict intestinal inflammation. Autophagy 17: 1096-1111, 2021.
79. Kuo WT, Zuo L, Odenwald MA, Madha S, Singh G, Gurniak CB, Abraham C and Turner JR: The tight junction protein ZO-1 is dispensable for barrier function but critical for effective mucosal repair. Gastroenterology 161: 1924-1939, 2021.
80. Kuo WT, Shen L, Zuo L, Shashikanth N, Ong M, Wu L, Zha J, Edelblum KL, Wang Y, Wang Y, *et al*: Inflammation-induced occludin downregulation limits epithelial apoptosis by suppressing caspase-3 expression. Gastroenterology 157: 1323-1337, 2019.
81. Guo H, Guo H, Xie Y, Chen Y, Lu C, Yang Z, Zhu Y, Ouyang Y, Zhang Y and Wang X: Mo(3)Se(4) nanoparticle with ROS scavenging and multi-enzyme activity for the treatment of DSS-induced colitis in mice. Redox Biol 56: 102441, 2022.
82. Wang R, Moniruzzaman M, Wong KY, Wiid P, Harding A, Giri R, Tong WH, Creagh J, Begun J, McGuckin MA and Hasnain SZ: Gut microbiota shape the inflammatory response in mice with an epithelial defect. Gut Microbes 13: 1-18, 2021.
83. Bakheet SA, Alrwashied BS, Ansari MA, Nadeem A, Attia SM, Assiri MA, Alqahtani F, Ibrahim KE and Ahmad SF: CXCR3 antagonist AMG487 inhibits glucocorticoid-induced tumor necrosis factor-receptor-related protein and inflammatory mediators in CD45 expressing cells in collagen-induced arthritis mouse model. Int Immunopharmacol 84: 106494, 2020.
84. Le HT, Golla K, Karimi R, Hughes MR, Lakschevitz F, Cines DB, Kowalska MA, Poncz M, McNagny KM, Häkkinen L and Kim H: Platelet factor 4 (CXCL4/PF4) upregulates matrix metalloproteinase-2 (MMP-2) in gingival fibroblasts. Sci Rep 12: 18636, 2022.

85. Kasirer-Friede A, Peuhu E, Ivaska J and Shattil SJ: Platelet SHARPIN regulates platelet adhesion and inflammatory responses through associations with αIIbβ3 and LUBAC. Blood Adv 6: 2595-2607, 2022.
86. Yu G, Rux AH, Ma P, Bdeir K and Sachais BS: Endothelial expression of E-selectin is induced by the platelet-specific chemokine platelet factor 4 through LRP in an NF-kappaB-dependent manner. Blood 105: 3545-3551, 2005.
87. Petrai I, Rombouts K, Lasagni L, Annunziato F, Cosmi L, Romanelli RG, Sagrinati C, Mazzinghi B, Pinzani M, Romagnani S, *et al*: Activation of p38(MAPK) mediates the angiostatic effect of the chemokine receptor CXCR3-B. Int J Biochem Cell Biol 40: 1764-1774, 2008.
88. Zeng B, Sun Z, Zhao Q, Liu D, Chen H, Li X, Xing HR and Wang J: SEC23A inhibit melanoma metastatic through secretory PF4 cooperation with SPARC to inhibit MAPK signaling pathway. Int J Biol Sci 17: 3000-3012, 2021.
89. Bonacchi A, Romagnani P, Romanelli RG, Efsen E, Annunziato F, Lasagni L, Francalanci M, Serio M, Laffi G, Pinzani M, *et al*: Signal transduction by the chemokine receptor CXCR3: Activation of Ras/ERK, Src, and phosphatidylinositol 3-kinase/Akt controls cell migration and proliferation in human vascular pericytes. J Biol Chem 276: 9945-9954, 2001.
90. Van Raemdonck K, Gouwy M, Lepers SA, Van Damme J and Struyf S: CXCL4L1 and CXCL4 signaling in human lymphatic and microvascular endothelial cells and activated lymphocytes: Involvement of mitogen-activated protein (MAP) kinases, Src and p70S6 kinase. Angiogenesis 17: 631-640, 2014.
91. Li LX, Xia YT, Sun XY, Li LR, Yao L, Ali MI, Gu W, Zhang JP, Liu J, Huang SG, *et al*: CXCL-10/CXCR3 in macrophages regulates tissue repair by controlling the expression of Arg1, VEGFa and TNFα. J Biol Regul Homeost Agents 34: 987-999, 2020.